Design of an electric motor (PMSM) & manufacturing lab.

HÖGSKOLAN I SKÖVDE

1977

Abstract

The thesis presents deals with the design, analysis, test and control of permanent magnet synchronous motor(PMSM).

An analytical model was carried out based on the d-q frame and the equivalent circuit of PMSM, the analytical model gives an approximation value of the machine parameters and is carried out by equations from the listed references. this phase includes many iteration steps, once the results were obtained they were compared with the motor specifications and if they don't match the required specifications the process must be done again until the desired design is obtained.

Once the analytical model is obtained a Finite Element Simulation was carried out using FEMM software to validate the design, in this phase the designed machine in the analytical model is analyzed and validated, once the simulation is done the results from both models are compared and discussed in the results chapter.

It's important to mark that during the design phase some design parameters were affected and limited by some factors, for example, the air gap length has been magnified due to manufacturing limits.
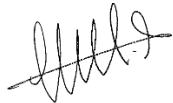
The manufacturing process and the prototype building have been started once the optimal design was selected, the manufacturing process was explained and a comparison study was made to select the best manufacturing process suitable and available for this thesis.

Keywords: Permanent magnet synchronous machine, PMSM, Finite element analysis(FEA), FEMM, Hairpin winding, Motor assembly, Prototype.

Certification

This thesis has been submitted by LAMA AWAWDA to the University of Skövde as a requirement for the degree of Bachelor of Science in Production/Mechanical Engineering.

The undersigned certifies that all the material in this thesis that is not my own has been properly acknowledged using accepted referencing practices and, further, that the thesis includes no material for which I have previously received academic credit.

Lama Awawda

Skövde 2021-05-12

School of Engineering Science

Table of Contents

1 Introduction

1.1 Background

Electrification and electromobility make it possible to reach the sustainability goals of the climate. But it requires the industry to change rapidly from the manufacturing of combustion engines to electrical drive lines. This swift change requires new competence, which can be provided by the University of Skövde. One of the required competencies that are requested is knowledge about the electrical driveline, and specifically manufacturing of electrical motors. There are courses today that include labs where the students disassemble and assemble a small electrical motor. This project is about designing a new lab including most steps in the manufacturing and testing of an electric motor. A new motor suitable for the lab will be designed and its performance needs to be evaluated.

Since the creation of the first rotary electric motors in the middle of the 19th century, to the present day, the participation of motors has been increasing in daily life. This is thanks to the most varied shapes, sizes, and construction techniques, in addition, of course, to the evolution of control and drive techniques, and increasingly indispensable, the embedded electronics that act as a link between the engine and the control system and drive.

Daily, motors are being used in various applications, these being industrial (robots, servo systems, automation), domestic (refrigerator, air conditioning, washing machines), commercial (computers, printers, scanners), transport (Trolebus, elevators, electric vehicles), equipment for the health area, air compressors, rehabilitation equipment), tooling (drill, emery), among others. (Gieras & Wing, 2002).

1.2 Sustainability

The designed motor of this thesis will be a motor for traction applications, therefore; the sustainability will focus on the sustainability of the electric motors of those applications.

Carbon Dioxide (CO_2) is considered as one of the most contaminated gas for the climate, a conventional combustion vehicle produces around 24 tons of Carbon Dioxide (CO_2) during its life cycle, while an electric vehicle produces around 18 tons. (LowCVP, 2015), many studies were realized on the effects of an electric vehicle on the climate and compare them with the effects on the conventional combustion vehicle, electric vehicles show that they could be a cleaner and more climate-friendly transport way.

The era of electric vehicles has begun. The Toyota Prius, a hybrid electric vehicle first introduced in Japan in 1997, was an initial milestone. By connecting a small generator and a rechargeable battery to the braking system of a normal car, the hybrid has, in addition to the normal engine, another powered by a battery. The mileage earned increases enough to make the hybrid commercially viable.

How electricity is obtained plays a decisive role in the ecological footprint of electric cars. When it comes to renewable energy, daily use has almost no impact on the environment. However, if conventional ways are used (which contain coal) to produce electricity, the footprint is significantly larger. Another factor influencing the environmental footprint of electric cars is the laborious and

CO2-intensive battery production. But even if conventionally produced electricity is taken into account for the calculation and production load is included, electric cars are still ahead.

1.3 Extent and Delimitation

The present work deals with the Design of an electric motor manufacturing lab. To start with the design, motor types and motors theory must be defined, due to the variety of the motor types and to be able to select the most suitable motor type for this thesis, the objectives and the specifications must be defined.

The pre-design stage of the motor to be carried out consists of the analytical and numerical calculation of the motor. The analytical calculation consists of the application of the mechanical and electrical equations of the motor. An iterative process is followed.

The advantage of the analytical calculation is the approximation to a specific model, although the precision of the results is not excessive. The numerical calculation consists of solving the equations of the motor through a finite element tool, capable of solving the exact differential equations applied to the motor.

In this way, the solution obtained is very precise, in exchange for a high calculation time, which closes the door to iteration until a suitable model is found. Therefore, in the search for the precision-calculation time, it is the combination of the two methods that leads to a good motor design: with the analytical calculation, a model close to the real one is obtained in a short time; and with the finite element program, the results are calculated accurately based on the analytical model, thus saving calculation time.

Next, the results will be analysed, comparing those obtained from the numerical calculation, with what was expected after the analytical calculation. Once the most suitable model has been selected. A final model will be designed, manufactured and tested in the designed lab.

1.4 Project Objectives

This thesis aims to design an electric motor suitable for assembly by hand since the assembly of the motor will be performed at the University of Skövde. A lab will be also designed which contain the assembly and disassembly processes stations and instructions, once the motor is designed and the prototype is mounted different tests and measurements will be performed to evaluate the motor performance and the feasibility to use the motor in the lab.

2 Theoretical Frame of Reference

2.1 Electric motor components

The electric machine's behaviour in its basic form is to convert energy from electrical energy to mechanical energy or vice versa; when the output energy is mechanical energy the machine is called a Motor, and when the output energy is electrical energy the machine is called a generator.

Working as a generator or as a motor, the electric machine basic components are (Kothari & Nagrath, 2010):
- The stator (the stationary part)
- The rotor (the rotating part)
- The shaft (the mechanical part which is responsible for the torque transmission)
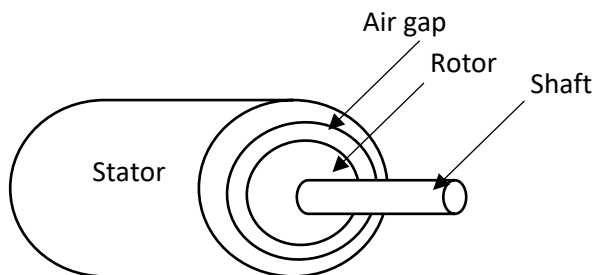
Figure 1 Electric motor parts, (Kothari & Nagrath, 2010)
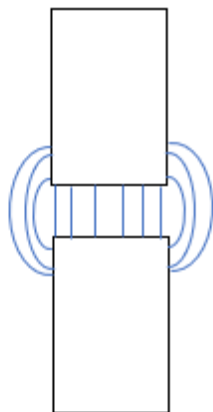
Between the rotor and the stator, there is the so-called air gap (Fig2); for electric machine designer the air-gap design is the most important design parameter, and that's because of the effects of its dimensions on the machine performance, for example, the air gap length can affect the reactance of the machine which affect other electric parameters and so the performance, there is an inverse relationship between the size of the air gap and the efficiency; therefore, a small air gap size is desired. (Hanselman, 1994).

Figure 2 Magnetic flux flow in an air gap between two highly permeable structures, (Hanselman, 1994)

Design parameters related to the air gap (slots, teeth, winding….etc) focus on the flux produced in the machine and they are related to each other with several equations which are defined in the motor design chapter, the relation between those parameters elevate the complexity of selecting and calculating their values, but if the designer can reach the optimal values, this could lead to high efficiency and high performance of the machine.

To be able to calculate the optimal values of those parameters, a deep theoretical study of electromagnetic relations and theory in electric machines must be done.

2.2 **Fundamental electromagnetic relations**

The electromagnetic field, which extends throughout space, comprises the electric and magnetic fields. The electric field is produced by static charges while the magnetic field is created by the movement of charges (currents) and represents the source of the field. The way these charges and currents interact with the electromagnetic field is described by Maxwell's equations and Lorentz's Law (Fleisch, 2008).

$$F_B = qv \times B \qquad \text{2-1}$$

Where:

- F_B: Magnetic force.

- q: Particle's charge.

- v: Particle's velocity.

- B: Magnetic field.

According to the Biot-Savart Law, the mathematical relationship between the magnetic field intensity H and the current I produced by the field is as follows:

$$\oint_L H.dl = I_{encl} = NI \qquad \text{2-2}$$

Where I$_{encl}$ is the enclosed current of the line integral, N is the number of turns and I is the current. While the product of NI represents the magnetomotive force (MMF). (Kothari & Nagrath, 2010). Magnetomotive force is the ability to creates a magnetic flux in a magnetic circuit and its unit is ampere-turn.

There is a direct relation between the flux density(B) and the magnetic field intensity (H), it's important to mention that this relation is related to magnetic permeability also (Kothari & Nagrath, 2010).

$$B = \mu_0\mu_r H = \mu H \qquad \text{2-3}$$

Where:
- μ_0: Vacuum permeability.
- μ_r: The relative permeability.
- B: The flux density.
- H: The field intensity.

The magnetic flux that is created by the magnetic field describes how much magnetic flux is flowing in a cross-section, it is described by

$$\emptyset = \int_A B.dA \qquad \text{2-4}$$

Here the integral is applied over the area of interest. by Ampere's law, the magnetic flux can be determined as the strength of the source of the magnetic field.

Electromagnetic induction, defined through the Faraday-Lenz Law, is the production of electric currents by time-varying magnetic fields. This phenomenon describes the existence of a magnetic field that will produce electric currents. In addition, the electric current increases by increasing the speed with which the magnetic flux variations occur.

Faraday explained the origin of this current in terms of the number of field lines crossed by the conducting wire circuit, which was later expressed mathematically in what is now called Faraday's Law.

Faraday's Law: "The electromotive force induced in a circuit is equal and of opposite sign to the speed with which the magnetic flux through a circuit varies, per unit of time." (Fleisch, 2008)

$$\varepsilon = -\frac{d\Phi}{dt} \qquad \text{2-5}$$

To determine the direction of an induced current, the so-called Lenz's Law is used, which stated that: "An emf gives rise to a current whose field opposes the change in flow that produces it." (Fleisch, 2008)

By the application of Ohm's law, the current density can be determined in function of the conductivity and the electric field intensity:

$$J = \sigma E \qquad \text{2-6}$$

Where:
- σ: conductivity of the material($\Omega^{-1}m^{-1}$)
- E: Electric field intensity(V/m).

2.3 Types of electric machines

As it's mentioned before, there are many motors types but the designed motor of this thesis will be a motor for traction applications, which reduce the types of motors to four main motors types that are used in traction applications:
- Induction motor (IM)
- Synchronous reluctance motor (SynRM)
- Brushless DC motor (BLDC)
- Permanent Magnet Synchronous Motor (PMSM)

The basic characteristics that must be met by an electric machine intended for traction application are as follows:
- High torque density and power density.
- High starting torque at low speeds.
- High efficiency over wide ranges of speeds and torque.
- Acceptable cost.

2.3.1 Induction motor(IM)

The induction motor or asynchronous motor is the most widely used electric motor in the industry, this is because of its simple construction process. The induction motor has a polyphase winding stator and its rotor can be constructed in two ways:

- Winding rotor
- Squirrel cage rotor
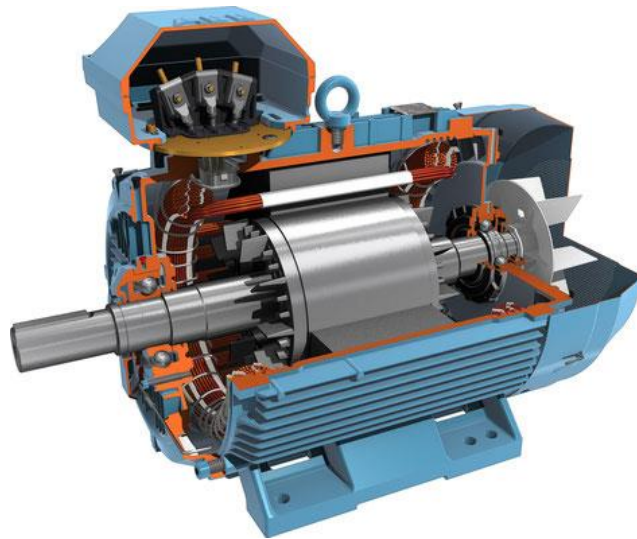
Figure 3 Induction motor (DistriMotor, 2020)

2.3.2 Synchronous reluctance motor(SynRM)

Synchronous reluctance motors are AC electric motors that combine a three-phase induction motor stator with a rotor, without windings or permanent magnets.

The (SynRM) utilizes the reluctance concept and rotating sinusoidal MMF for torque production.

Figure 4 SynRM (chile, 2017)

2.3.3 Brushless DC motor(BLDC)

The BLDC motor is a variant of the brushed DC motor, as this motor eliminates the brushes that lead to eliminating the limitations that the collector assembly gave. These motors have been able to improve their performance after eliminating the brushes since they gave losses due to scrubbing.
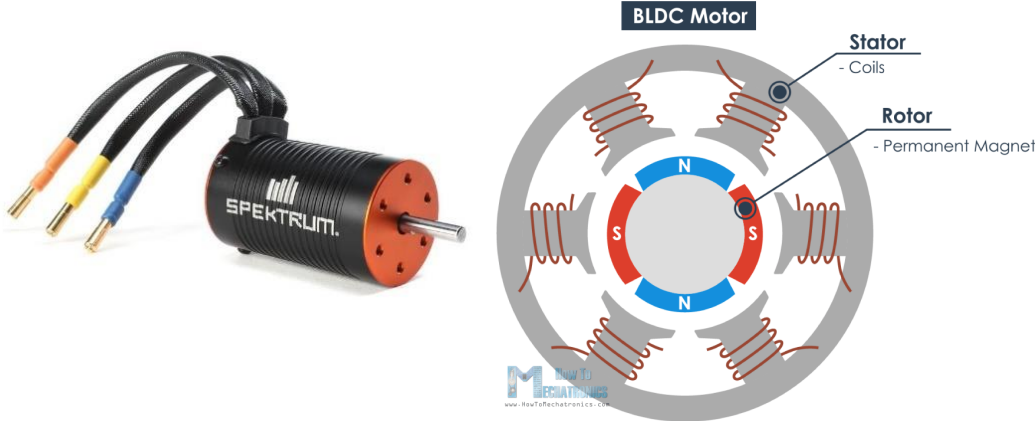
Figure 5 BLDC (Spektrumrc, 2021) (Mechatronics, 2019)

2.3.4 Permanent magnet synchronous motor(PMSM)

The PMSM is made up of a stator in which it has a polyphase alternating current winding and a rotor where the permanent magnets are housed, which create a stationary magnetic field in the air gap.

Figure 6 PMSM (Nogueira, 2013)

2.4 **Basic characteristics of the electric machines**

The following table shows the basic characteristics of the discussed machines:

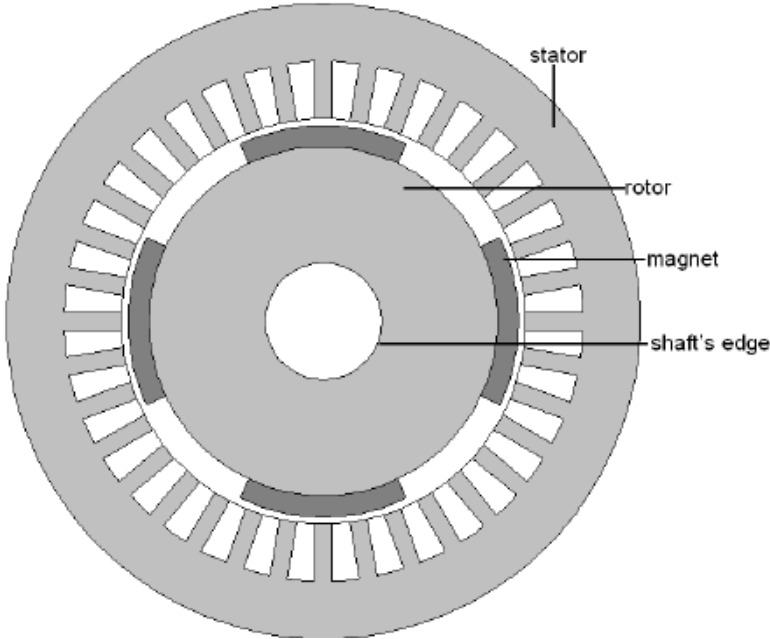|	Induction motor (IM)	Synchronous reluctance motor(SyRM)	Brushless DC motor (BLDC)	Permanent Magnet Synchronous Motor (PMSM)
Basic features	• Robustness. • low construction cost. • Good response to overloads. • Good speed range.	• Low-cost materials • Constant speed under all circumstances. • Robustness. • Reliability.	• High power density. • High performance. • Low maintenance.	• High power density. • Low Joul losses. • Wide range of speeds. • High performance.
Disadvantages	• High rotor copper losses. • Low efficiency in small size machines.	• Difficulties in speed control. • High torque ripple. • Poor power factor.	• High cost. • Resonance.	• High cost of rare-earth magnet. • Magnets' characteristics tend to change over time

Table 1basic characteristics of the electric machines.

2.5 **PMSM theory**

The evolution of permanent magnet machines has risen with the development of magnetic materials. The materials known as permanent magnets are those that have a high magnetic energy storage capacity, which lasts for a long time.

The introduction of permanent magnet machines takes place in 1973, even though there are antecedents such as direct current machines of the mid-nineteenth century, which used remanent magnetism. These machines appear as a result of the discovery of a new alloy, Al-Ni-Co; although it was somewhat limited to small machines, as well as analogous materials such as ferrites since the magnetization was not too high.

In the 1970s, a rare earth magnet was discovered, which prompted the development of larger machines. In 1980, a new alloy with magnetic properties was developed, Nd-Fe-B, and these materials began to be developed until their prices fell as a consequence, which allowed them to expand their field of applications.

2.5.1 Permanent Magnet (PM)

Permanent magnets are materials that are magnetized and can persistently generate their magnetic field. The fundamental difference between them and an electromagnetic magnet is that the latter only generate a field while the external force that causes it is acting.

They are characterized by their hysteresis curve. The hysteresis curve of a material is the curve that defines its magnetization, facing magnetic field (H) and magnetic induction (B); it is particular to each material. One of the properties of permanent magnets is that their hysteresis curve is especially wide, which gives high values of B and H therefore higher flux density can be produced in the air gap.

Types of permanent magnets:

The classification that can be made of permanent magnets is between artificial and natural magnets:

- Natural permanent magnets: due to their high cost, they are the least used.
- Artificial permanent magnets: are obtained from hard ferromagnetic materials, which once magnetized, tend to maintain their magnetic properties until they are demagnetized.

The most important compounds in the manufacture of permanent magnets are:

a) Alnico: It is an alloy of cobalt, aluminium and nickel. Sometimes iron, copper or even titanium are also added.
b) Ferrite: also known as iron-α, since it comes from crystallized iron in the cubic system under specific temperature conditions.
c) Neodymium: an alloy of neodymium, iron and boron (Nd-Fe-B). They are the so-called rare earth magnets; They are characterized by having a high coercive field value and remanent induction (which makes them the ones with the highest performance).
d) Samarium-Cobalt: PMs made of this alloy also belong to the group of rare earth magnets, although they are less commercialized than Nd-Fe-B.

The properties of these materials can be explained through the study of their hysteresis curve. The hysteresis curve shows the relationship between the magnetic field (H) and magnetic induction (B) and is generated by measuring the magnetic flux of a ferromagnetic material while the magnetizing force is changing. the greater the magnetizing force, the stronger the magnetic field B in the material.
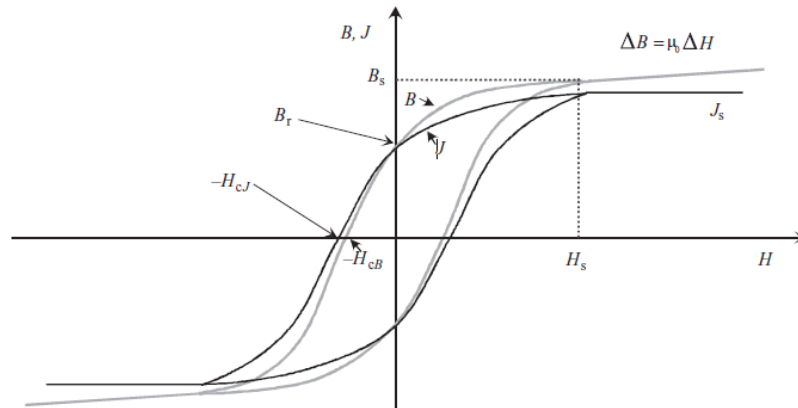
Figure 7 Hysteresis curve (Pyrhonen, et al., 2008)

	Ferrite	Alnico	Sm-Co	Nd-Fe-B
Remanence, B_r (T)	0.43	1.25	1.21	1.47
Coercivity, H_C (Ka/M)	330	51	796	820
Energy product, $(BH)_{max}$ (KJ/m³)	35	44	271	422
Temperature coefficient of Br (%/°C)	-0.18	-0.02	-0.03	-0.11
Temperature coefficient of H_C (%/°C)	0.2	0.01	-0.22	-0.65
Curie temperature, Tc(°C)	450	860	825	345

table 2 Properties of PM materials (Chau, 2015)

2.5.2 Permanent magnet synchronous machine operation
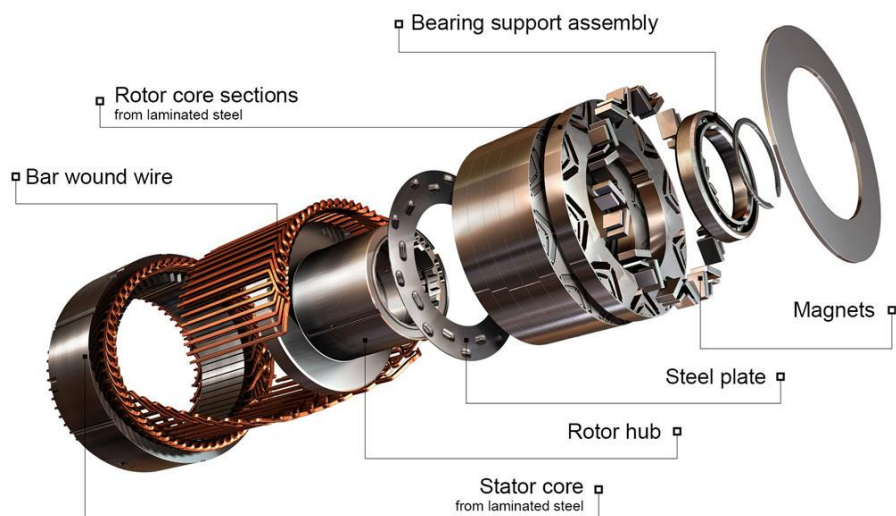
Figure 8 PMSM components (Levkin, s.f.)

A permanent magnet (PM) motor is an AC motor that consists of a rotor with permanent magnets embedded into or attached to the surface, while the stator of PMSM is the same stator of an induction machine; where 3 phase winding is placed in the stator slots, the rotation action of this machine is produced by the interaction between the rotating magnetic field produced by the stator winding and the stationary magnetic field produced by the permanent magnet of the rotor. PMSM is an AC synchronous machine which means that the rotor is rotating at the same speed as the stator's rotating field.

The induced electromotive force(emf) in the armature is the resulting voltage due to the relative motion between the rotor flux and the stator conductors, the 3 phase emf can be expressed as follows (Chau, 2015):

$$e_a = E_m \sin(\omega t) \qquad\qquad 2\text{-}7$$

$$e_b = E_m \sin(\omega t - 120°) \qquad\qquad 2\text{-}8$$

$$e_c = E_m \sin(\omega t - 240°) \qquad\qquad 2\text{-}9$$

And the current is a balanced three-phase sinusoidal system which can be expressed as:

$$i_a = I_m \sin(\omega t - \theta) \qquad\qquad 2\text{-}10$$

$$i_b = I_m \sin(\omega t - 120° - \theta) \qquad\qquad 2\text{-}11$$

$$i_c = I_m \sin(\omega t - 240° - \theta) \qquad\qquad 2\text{-}12$$

Where:

-   I_m: The amplitude of the current waveform.
-   E_m: The amplitude of back EMF waveforms.
-   ω: The angular frequency.
-   θ: The phase difference between the current and back EMF waveforms.

The electrical power of PMSM can be calculated as follows:

$$P_e = e_a i_a + e_b i_b + e_c i_c = \frac{3E_m I_m}{2} \cos\theta \qquad\qquad 2\text{-}13$$

After the power is calculated the developed torque is expressed by:

$$T_e = \frac{P_e}{\omega_r} = \frac{3E_m I_m}{2\omega_r} \cos\theta \qquad\qquad 2\text{-}14$$

Where:

ω_r: Rotating speed.

As can be noticed from equation (2-14), the torque value can be maximized by adjusting the phase difference between the stator current and the emf waveforms, the maximum value of the torque will be obtained when the difference is equal to zero.

the produced torque in a PMSM has two components the magnetic torque and the reluctance torque, the reluctance torque is produced due to the alignment of the rotor permanent magnet to the stator teeth, while the magnetic torque is the responsible torque of the machine rotation and it's produced due to interaction between the permanent magnet's flux field and the current in the stator winding."

2.6 **PMSM rotor configurations**

PMSMs has different rotor configurations, the topologies are classified depending on where the magnets are located, and the configurations are selected depending on the application of the machine, the most important rotor types are shown in the following graphic:
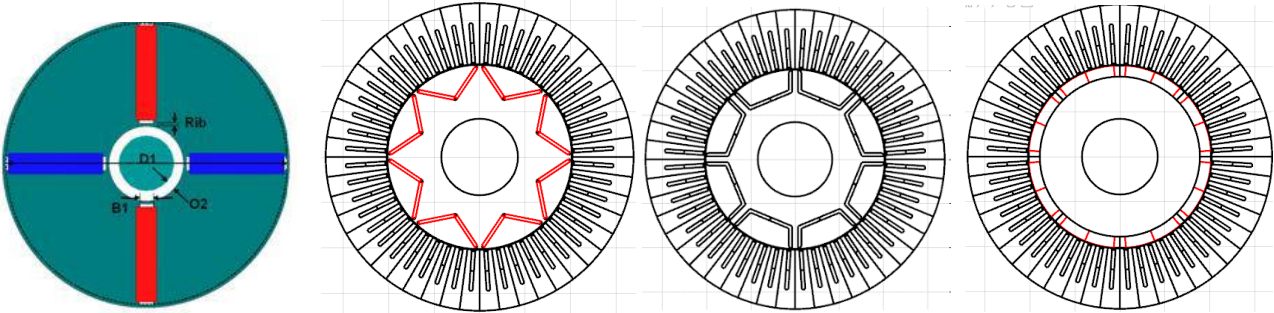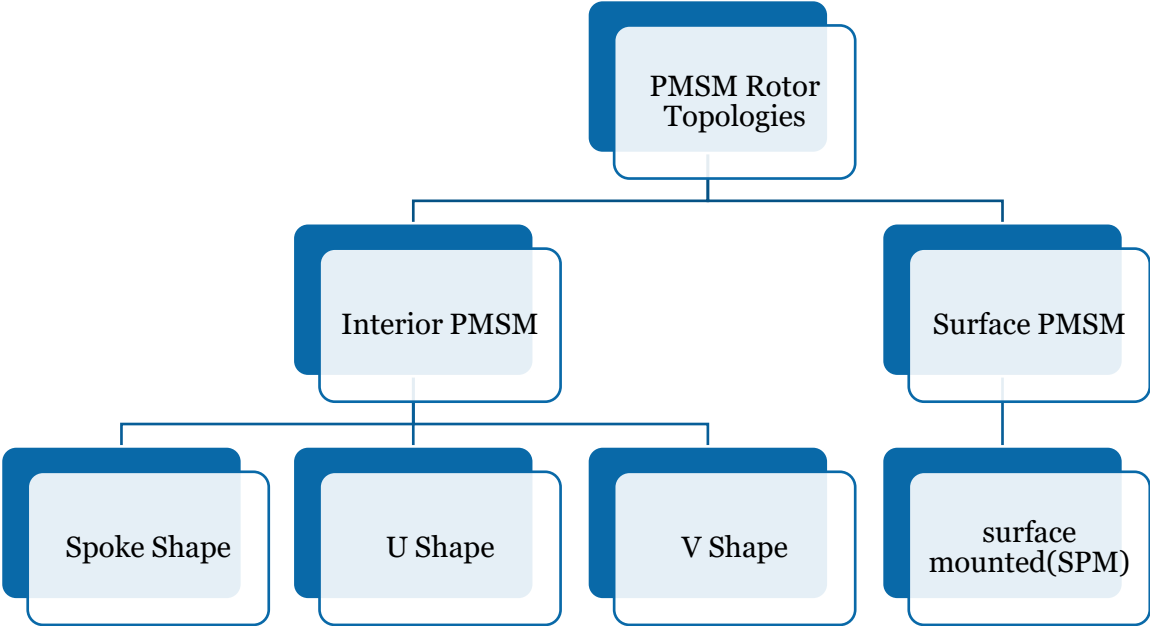

Figure 9 Rotor topologies(Spoke shape, V shape, U shape, SPM)(SyR-e Software)((Namitha, et al., 2020).

The main characteristics of the mentioned rotor shape are listed in the following table (MARTÍNEZ, 2012):

Surface PMSM	Interior PMSM
PMs are located in the rotor surface	PM is located inside the rotor slots
Lower cost	High air gap flux density
Simplicity of construction	Protected against demagnetization and mechanical stress
It exposes the PM to demagnetization fields	Complex designs
	Higher cost

table 3 Main characteristics of the rotor shapes.

2.7 **Losses**

Losses in an electric motor are defined as the difference between the input power and the output power, in the case of the motor the input power is the electrical power, and the output power is the mechanical power on the shaft.

Electric motor losses are discussed in this chapter:

2.7.1 Copper losses

As a general rule, copper losses are usually the largest. They are caused due to the Joule effect, and they depend on the current circulated through the stator windings and their temperature. (Wildi, 2002)

The main equation for calculating the copper losses in a phase is very simple (Hendershot & Miller, 1994):

$$P_{cu} = R_{phase} * I^2 \qquad \text{2-15}$$

Where (I) is the phase current and (R_{phase}) is the resistance of phase A winding. To calculate the resistance:

$$R_{phase} = {}^l\!/_{\sigma_{cu} * S} \qquad \text{2-16}$$

Where l is the length of the copper that makes up the entire phase (m), S is the section in (mm2) of the conductor and σ_{cu} is the conductivity of the copper. The conductivity of copper is temperature-dependent and is defined as

$$\sigma_{cu} = \sigma_{20°} * (1 + T - 20) * \alpha_{20°} \qquad \text{2-17}$$

With the equations that have been presented, the direct component losses will be calculated. But it must also pay attention to the phenomenon that appears when an alternating current flow through a conductor: the skin effect. It is the tendency that alternating currents have when they circulate

through a conductor to be distributed within a conductor in such a way that the area near to the surface contains a current density greater than inside the conductor. That is, the current tends to flow through the surface of the conductor. The skin effect increases the resistance of the conductor with frequency.

2.7.2   Iron losses

On the other hand, Electric motors have losses in iron produced in the magnetic core of the machine. These losses, caused by hysteresis and eddy currents, increase with speed and are generally the second-largest source of losses.

Hysteresis is a phenomenon that appears in ferromagnetic materials, which produced because of the loss of energy each time a hysteresis loop is traversed.
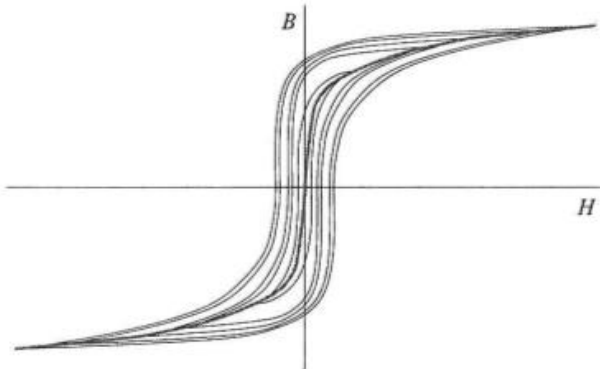
Figure 10 Ferromagnetic material magnetization characteristics (Hanselman, 1994).

To be able to reduce those losses a magnetic material of a narrow hysteresis loop must be selected. (Wildi, 2002).
Eddy currents losses are a result of Faraday's law; which states" the motion of a conductor exposed to a magnetic field produces a current which produces internal magnetic fields that oppose the change". In PMSM eddy current is produced when the motor core rotates in the magnetic field, which induce an EMF in the coils and as a result current is circulating referred to as eddy currents. To reduce eddy currents the motor cores are made of very thin pieces o iron (lamination), in this way the resistance of the cores increases which cause the reduction of the circulating eddy current, the core laminations are also insulated from each other to prevent the eddy currents from moving from one lamination to another.

Figure 11 Eddy currents in laminated core *(Collins, 2018).*

In general, Iron losses are described by:

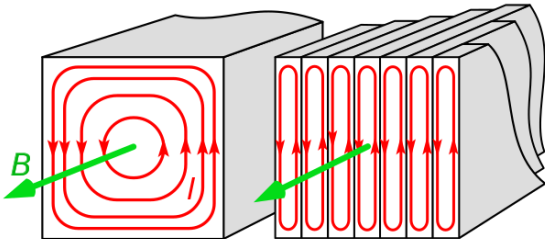$$P_{fe} = \frac{1}{\gamma}\left(K_h f B^2 + K_c f^2 B^2 + K_a \sqrt{f^3 B^3}\right) \qquad \text{2-18}$$

Where:
- γ: Specific iron density.
- B: Flux density.
- f: Frequency.
- K_h, K_c, K_a: Coffecienct of the lamination material.

2.7.3 Magnet losses

Magnet losses are caused due to two factors: temperature and eddy currents. Magnets lose their properties with increasing temperature and eddy. currents Special attention must be paid to Eddy currents as they can be a major source of losses, and what is worse, they can lead the magnets to irreversible partial demagnetization.

2.7.4 Mechanical losses

These losses are usually due to friction in bearings with bearings and friction with the air.

2.8 Cogging torque

Cogging torque is the produced torque when the rotor tries to align with the stator teeth due to the PM, this torque is not desirable in PMSM because it causes variations in the total torque produced by the machine and cause noise and vibrations in the machine.

Cogging torque highly depends on the number of the stator teeth and the rotor PMs and the ratio between them, and it can be decreased by optimizing the ratio between them, or by skewing or shaping the permanent magnets to make their transition between stator teeth more gradual.

Ripple torque is the result of cogging torque, and it's referred to as the variation of torque production, torque ripple varies sinusoidally. At high speeds, ripple torque can be filtered out by the inertia of the system, but at lower speeds, it may cause unwanted speed fluctuations, vibrations, and audible noise.
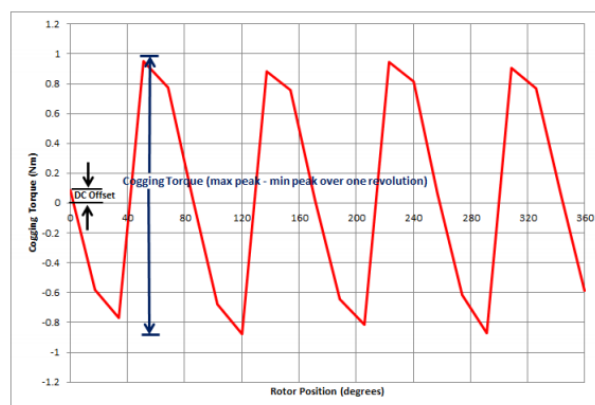

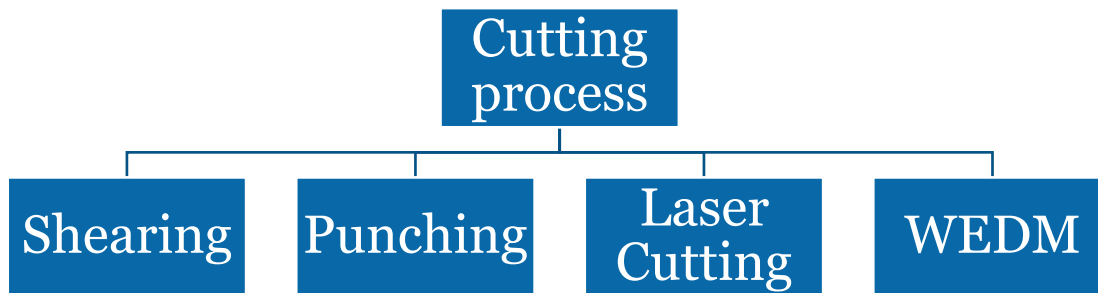*Figure 12 Typical cogging torque waveform (IEEE, 2021)*

2.9 **The electric motor manufacturing process**

After the selection of materials and the selection of the desirable design of the motor, the manufacturing process starts; the main manufacturing process of an electric machine is related to the cores of the machine (stator and rotor laminations). Regarding (Sarrico, 2017), Three main manufacturing process are used in motor manufacturing:

- Cutting process.
- Stacking process.
- Winding process.

2.9.1 Cutting Processes:
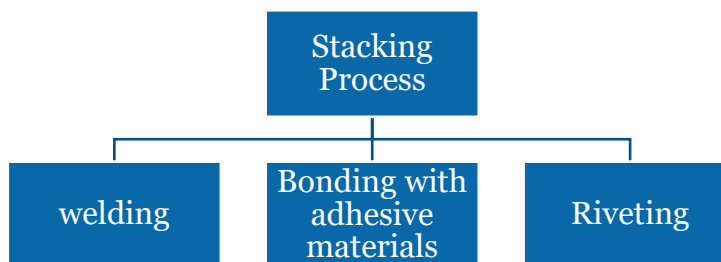
Five cutting process methods are defined:

```
                    Cutting
                    process
    ┌──────────┬───────┴────────┬──────────┐
 Shearing   Punching    Laser Cutting   WEDM
```

- **Shearing**: method can be defined as a fabrication mechanical cutting process that's used to perform certain cuts in a material (Paper, Wood, Metal sheets...etc). the shearing method is realized by the use of a tool or machine; this method doesn't produce waste in form of chips, it's a very fast method, it can create clean cuts and it can be performed at room temperature since it doesn't need any use of heat; this method may cause deformation in the material.

- **Punching**: in punching cutting a shear force is applied to perform the cutting action, mainly used to process holes into flat materials like metal sheets, paper or plastic film. It's easy to use and it has a lower operating cost. It's also fast, Punches could be a noisy process, that can be dangerous for the user.

- **Laser Cutting:** laser cutting apply the laser to cut the material, this method is widely used and it's considered one of the most used methods for the lamination cutting process, the process consists of applying laser on the material which causes rapid heating, melting and partial or total vaporization of the material. The material zone exposed to the laser is small which means that the cut pieces show minimal deformation. on the other hand laser cutting is safe to use and offers a high cutting precision, in some cases the cost can be an issue if a lot of energy is consumed.

- **Wire Electric Discharge Machining (WEDM)**; in this method, the cutting process is performed by chip removal, the electric arc is generated to remove particles from the material until the shapes of the electrode are reproduced. even though this method can provide a very good finishing but it could be time-consuming depending on the design and the amount of material that has to be removed.

(Wenmin, et al., 2014) concluded that mechanical cutting methods as punching and shearing can negatively affect the magnetic properties of the materials and it produces stress and strain in the cut edge, while laser cutting shows the highest iron losses of the specimen, but its magnetic induction is the lowest. On the other hand, WEDM and water jet cutting gave better results regarding the effects on the magnetic properties and there is no stress or strain in those methods.

2.9.2 Stacking process

After the cutting process, the metal sheets must be stacked together to form the cores, the stacking process is related and can affect the motor proficiency; some stacking technologies can increase motor iron losses or affect the magnetic properties of the materials; the most common technologies are analysed in this part:

```
                    Stacking
                    Process
                       |
        ┌──────────────┼──────────────┐
     welding      Bonding with      Riveting
                    adhesive
                    materials
```

- **Welding**: it consists of welding all the sheets together. Regarding (Krings, et al., 2014); the welding process has negative effects on the laminations, it destroys the thin insulation layer between the lamination sheets, which causes short-circuit paths. Increasing eddy current losses. In addition, it also affects the hysteresis losses due to the induced thermal and mechanical stresses in the steel sheet lamination.
- **Bonding with adhesive materials**: This process consists of the joining of the surfaces by the use of glue, epoxy…etc, this method doesn't increase eddy current but it provides low mechanical strength.
- **Riveting/Bolting**: This process consists of the joining of two metallic parts by the use of rivets or bolt, this method doesn't change the physical structure of the materials, this method is quite cheap.

2.9.3 Hairpin winding

In PMSM the machine is working due to the interaction between the rotor field and the stator field, as mentioned before the rotor field is produced by the permanent magnet while the stator field is produced by the winding in the stator slots, choosing a winding type is very important since the machine performance highly depends on it, for example, the value of copper losses is affected by the winding type and it can significantly reduce or increase the efficiency of the machine.

Hairpin winding is a new development, but the attention is increasing to use it due to its beneficial electromagnetic and thermal performance, in hairpin winding a high fill factor can be achieved for its rectangular shape wire and the greater is the filling factor the lower is the copper loss and therefore a higher efficiency is achieved.
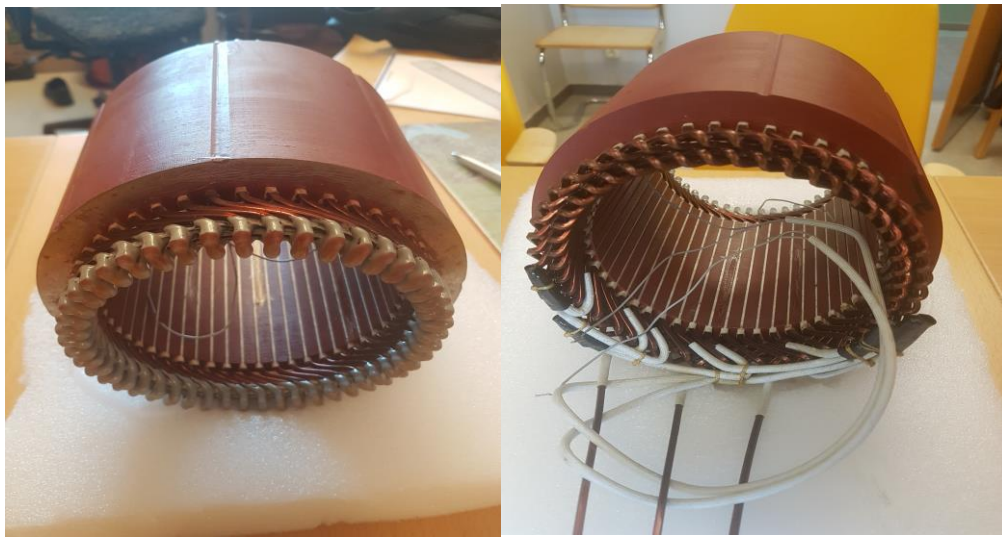

Figure 13 Fully assembled hairpin stator from Chalmers' hairpin machine (Deurell & Josefsson, 2019)
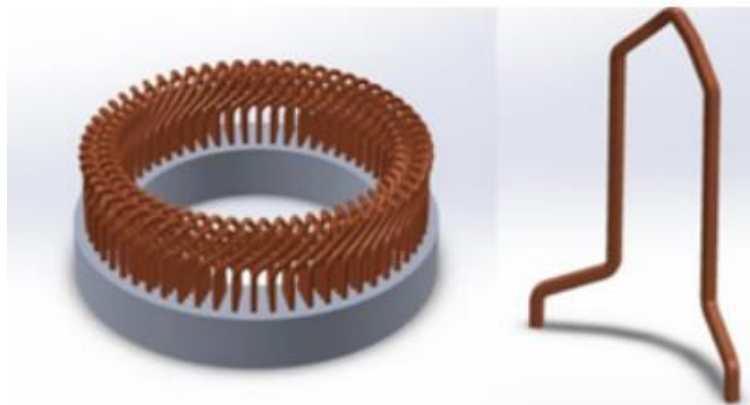

Figure 14 Hairpin winding in an electrical machine (Limited, 2021)

Hairpin windings consist of solid copper conductors which are bent into a so-called "hairpin shape", once the hairpin shape is formed, it inserted into the stator slots to form the winding, the legs of the hairpin wire is then bent again and welded with another hairpin wire to form a coil, the winding assembly process will be explained in the assembly chapter, the following table shows some advantages and disadvantages of hairpin winding (Limited, 2021):

Advantages	Disadvantages
High Fill Factor	Higher cost
Good thermal performance	Less flexibility

table 4 Advantages and disadvantages of hairpin winding

3 Literature Review

The design and optimization of the machine developed here have some works as references, including textbooks, articles, and thesis. The textbooks, mainly, gave a theoretical basis of the machine's design and most of the formulations that make it possible to dimension this machine, in addition to indicating some paths and possibilities for its optimization. The articles, together with the thesis, provided an excellent knowledge base for the optimization of the project, serving in many cases, as a reference point for the determination and combination of parameters to achieve the best result in a specific aspect.

In (Jape & Thosar, 2017)a comparative study of electric motors was realized, the authors compared different types of motors based on certain parameters which should be considered for the selection of the motor type. The article also shows some characteristics graph of the motors. It concludes the reluctance synchronous motor as a great alternative to induction motor and BLDC motor with a lower cost of motor and controller, high efficiency, reliability, and fault tolerance capability. But it also concludes that the Synchronous motor has higher efficiency at lower speeds and improves battery utilization and driving range for electric vehicle applications.

In (Jagasics & Vajda, 2016)a comparative study of PMSM with different rotor configuration were discussed, a comparison study of different parameters like performance characteristics, current performance, torque density and magnetic flux densities of the different rotor configurations were done. This article shows that the spoke type rotor geometry is the optimal shape of the analysed rotor versions.

In (Hendershot & Miller, 1994)a whole study of the design and dimensioning of synchronous permanent magnet machines was done. The authors highlight several aspects that must be observed in the dimensioning of each component of the machine, from the thickness of the magnet, thickness of the tooth, length of the air gap, to the distribution of the coils in the machine. They define guidelines for the construction of motors and link a series of formulations that give a first estimate for the dimensioning of the project.

Just as (Hendershot & Miller, 1994), in (Hanselman, 1994), dimensional aspects of motors are also addressed. However, in the latter, the study is initiated and carried out more superficially. In one aspect or another, the author goes into more detail but maintains the generic approach to give an overview of the constructive aspects of such machines.

In (Gieras & Wing, 2002), the approach differs from the aforementioned authors. The study is aimed at presenting and comparing the technologies of permanent magnet motors, a comparison made with other machines such as induction and switched reluctance motors, demonstrating the advantages of machines that use a permanent magnet as a source of excitation.

Concerning studies on permanent magnets, their evolution, and their use in motors, (Nasar, et al., 1993)makes a detailed study and brings simulation algorithms for magnetic circuits and finite elements. This helps to define the Finite element analysis and simulation steps for project validation.

In (MARTÍNEZ, 2012) there is a complete project for a Permanent-Magnet Synchronous Machine design. An analytical design was done first, after that, the machine calculated in the analytical model is evaluated. This evaluation is carried out through the use of an own-developed program based on the Finite Element Method Magnetics package (FEMM). It also highlights the advantages of concentrated windings type. This project as with many other thesis serves as a reference point for the design steps of the motor.

4 Method

This thesis carries two design directions, the motor design then the lab design, in this chapter the methodology used for the design of the electric motor and the design of the lab were done. Regarding the design of the motor; A list with several steps, enumerated, must be carried out to design a motor found in (Hendershot & Miller, 1994). Here, however, we will not strictly follow this list, that is, in the same order, since the order found in this work, does not always follow a sequence consistent with what was done in the previous step. Based on the studies carried out in the works of (Gieras & Wing, 2002), (Hanselman, 1994), (Hendershot & Miller, 1994) and (Nasar, et al., 1993) a clearer and more coherent list of steps are created, to have a more succinct order about the development of the project.

4.1 Machine design

1. Motor type selection
2. Rotor topology selection.
3. Material selection.
4. Electrical model
5. Analytical model
6. Numerical model(FEM analysis)
7. Parametric adjustments, if necessary, and repetition of the simulation.
8. Selection of the final design.
9. Build the selected design (prototype building)
   a) Cutting process.
   b) Stacking process.
   c) Winding of the stator.
   d) Motor assembly.
10. Assembly instructions & tests selection.

4.2 **Lab design**

Regarding the lab design, a list of design steps is defined:
1.   Define the measurements and tests to be realized on the designed motor.
2.   Define the necessary instruments and equipment for the tests.
3.   Design a lab manual (assembly instructions).
4.   Selection and purchase of instruments and equipment.
5.   Build the designed lab.
6.   Run and evaluate the lab.

4.3 **Evaluation of the manufacturing lab**

Regarding (Berman, 1979), the evaluation of a laboratory is an examination of its ability to perform a specific test, the evaluation method should provide information on its systematic errors, its ability to replicate its measurement, and the probability that the quality of laboratory performance will be maintained. The evaluation of a laboratory can be done by the use of one of those three methods:

- Data collection.
- On-site inspection of the laboratory.
- Proficiency tests.

For this thesis, the first method (Data collection) was chosen, this method could be realized by the use of student reports, surveys, or by interviews (Josselin & Le Maux, 2017), unstructured or semi-structured interviews with the students could be the fastest method to evaluate the lab.

5 **Machine design**

In this chapter the analytical, electrical and numerical models were carried out, first of all, the electrical model was obtained using the (d-q) frame then the analytical method was obtained using assumptions, equations and design steps found in the listed references in the literature review, the numerical method was performed by applying the finite element analysis to the designed machine obtained from the analytical model, the combination of the finite element method and the analytical method gives very accurate results and a validated machine since the analytical method can't provide an accurate design and some parameters equations are highly complex to be calculated in the analytical model, therefore, the FEM is used to validate the design obtained from the analytical method.

5.1 **Motor type selection**

Permanent Magnet Synchronous Motor was selected since it seems to be the best option for the thesis purpose, and according to (Fernández, 2014), PMSM shows the highest score of the selection matrix.

Property:	PMSM	SRM	SynRM	IM	DCM	EMSM	Weight
Cost (incl electronics)	2	4	4	4	3	4	5
Weight	5	4	4	4	3	3	5
Size	5	4	4	4	3	4	4
Inertia	4	5	4	4	3	4	3
Acoustic noise level	4	2	4	4	4	4	5
Electric noise level	5	3	4	4	3	4	3
Response time	5	5	4	5	5	5	3
Control accuracy	5	4	4	4	4	5	3
Torque	5	4	3	4	4	4	3
Efficiency	5	4	4	4	2	4	4
Power	5	3	3	3	2	4	4
Speed range	4	5	5	5	3	5	4
Fail safety	3	5	5	5	5	5	4
Drag torque	4	4	4	4	4	4	3
Complexity of electronics	4	4	4	4	5	3	3
Complexity of software	4	3	3	3	5	3	3
Cooling capabilities	5	4	4	3	3	3	4
Temperature restistance	3	4	4	4	4	4	4
Maintenance	4	4	4	4	2	3	2
Technical risk	5	4	4	5	5	4	2
Total score	301	278	282	286	251	281	

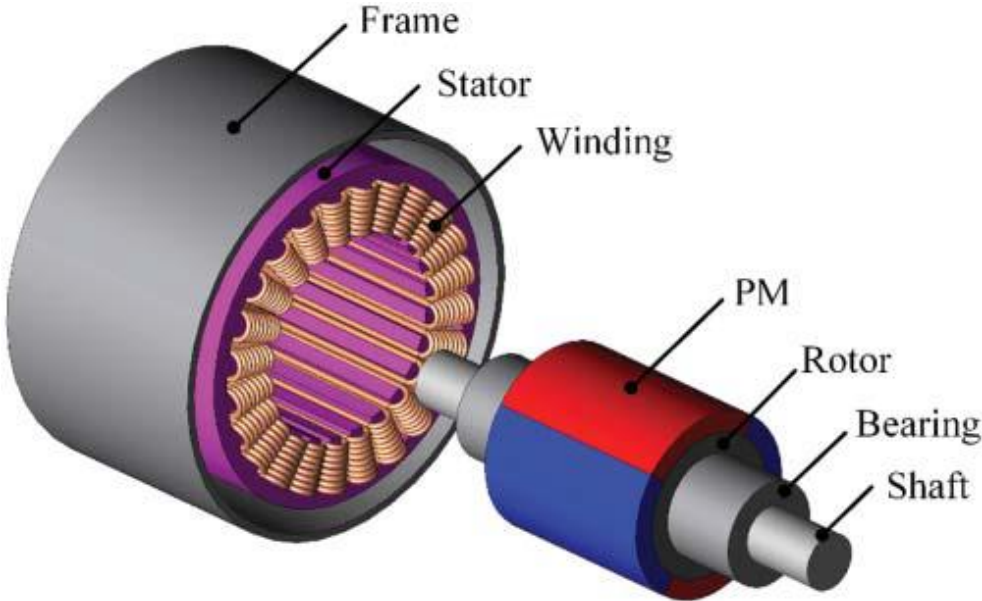*Figure 15* Machine Selection Matrix *(Fernández, 2014)*.

Figure 16 PMSM Components *(Chau, 2015)*.

5.2 **Rotor topology selection**

V-shape was selected for PMSM since it shows the high efficiency with less weight, low cogging torque and better current performance (Murali, et al., 2020).
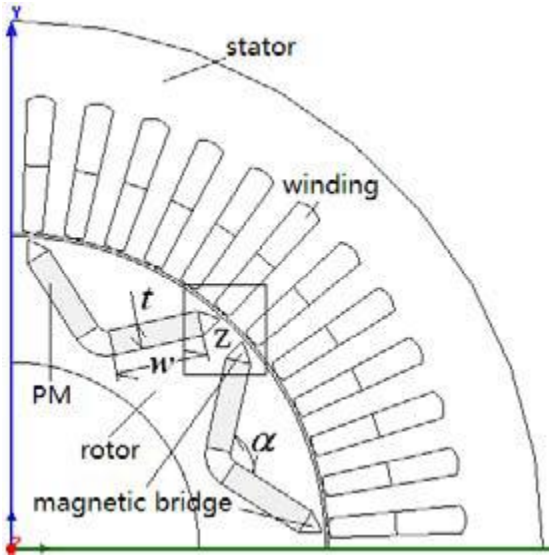

Figure 17 Model of V-shape IPMSM *(Huijuan , et al., 2013)*

5.3 **Material selection**

5.3.1 **Permanent magnet selection**

The selected magnet is the neodymium magnet (NdFeB N45M), this magnet is considered a strong magnet with the highest values of Magnetic remanence and Coercivity which helps to reduce the machine size.

table 5 NdFeB N45M Parameters.

Parameters	Symbol	Value	Unit
Magnetic remanence	B_r	1.33	Tesla
Coercivity	H	987	KA/m

5.3.2 Conductor material

For the winding wires the copper was used, which presented the following characteristics:

table 6 Copper wire parameters.

Parameters	Symbol	Value	Unit
Relative permeability	μ_0	1	N/A²
Electrical conductivity	σ	58	MS/m

5.3.3 Cores materials

The lamination sheet that used to form the motor cores are made of the M530-65A sheet, which has the following parameters:
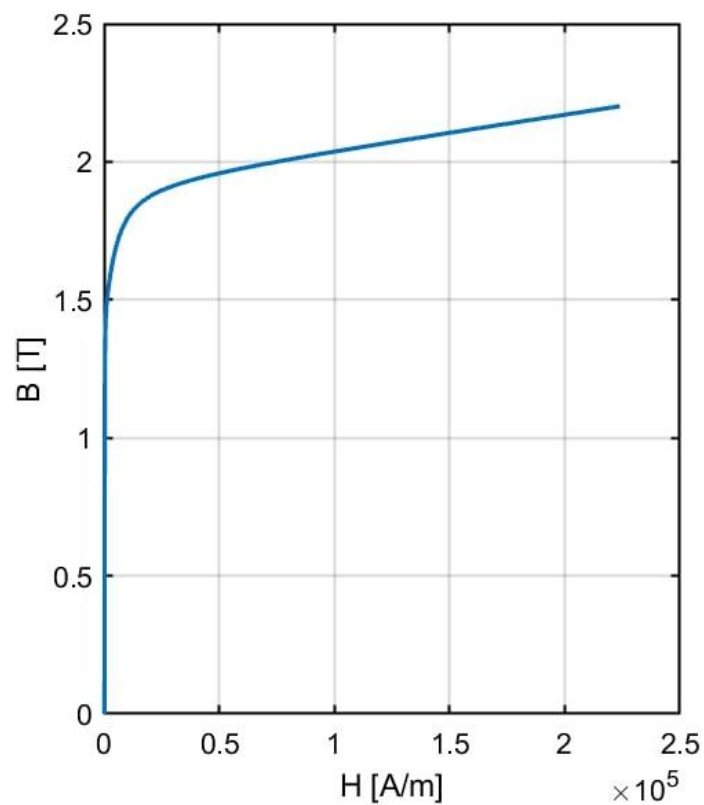

Figure 18 B-H Curve(FEMM)

- Mass density: 7700 kg/m³.

5.3.4 Shaft material

For the motor shaft material the stainless steal 316 was selected, the characteristics of this material are listed in the following table:

Parameters	Value	Unit
Density	8	g/cm³
Malting point	1400	°C
Elasticity module	193	GPa
Thermal conductivity	16.3	W/m.K
Electrical resistivity	0.074 *10⁻⁶	Ω.M

table 7 Shaft material parameters.

5.4 Electrical model

The electrical model of the machine was performed using the d-q coordinate based equivalent circuit (Qinghua2005 ‹), the following figure shows the equivalent circuit of PMSM.
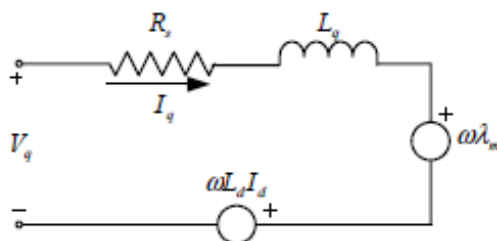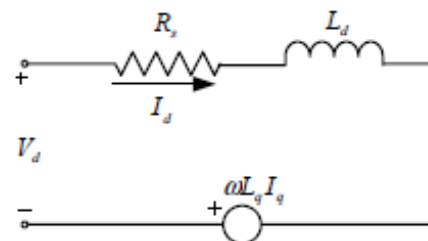

Figure 20 q-axis circuit   Figure 19 d-axis circuit

The electrical dynamic equations can be written as follows:

$$v_d = R.i_d + \frac{d\emptyset_d}{dt} - \omega_r \emptyset_q \qquad \text{5-1}$$

$$v_q = R.i_q + \frac{d\emptyset_q}{dt} - \omega_r \emptyset_d \qquad \text{5-2}$$

Where the fluxes equations are:

$$\lambda_d = \emptyset_m + \emptyset_d = L_d i_d + \emptyset_m \qquad \text{5-3}$$

$$\emptyset_q = \emptyset_q = L_d i_q \qquad \text{5-4}$$

Where:

- $\emptyset_m$: Permanent magnet flux.

The equations in the steady-state are:

$$v_d = R.i_d - \omega_r L_q i_q \qquad \text{5-5}$$

$$v_q = R.i_q + \omega_r L_d i_d + \omega_r \emptyset_m \qquad \text{5-6}$$

$$T = -\frac{3}{2}.p\left(\emptyset_d i_d - \emptyset_q i_q\right) = -\frac{3}{2}.p\left(L_d - L_q\right)i_q i_d + \emptyset_m i_q \qquad \text{5-7}$$

The torque has two components, the one due to the interaction between the flux of the magnets and the q component of the current and the reluctance component as a consequence of the difference between the inductances of the d-axis and the q-axis.

5.5 **Analytical model**

The analytical method is used to determine the electric and magnetic properties that define the motor geometry and dimensions, in this design phase important parameters of the motor were selected and the analytical model was built starting from the electrical and mechanical characteristics. The design steps and equations were selected from the references mentioned in the literature frame.

5.5.1 Specifications and machine characteristics

The characteristics required for the machine must be the first step of the design since depending on the application the characteristics may differ and therefore the design steps. For this (Chau, et al., 2008) describes the necessary characteristics of the electric machines for traction applications:

- High efficiency.

- Wide torque and speed range.

- High torque and power density.

- Low acoustic noise.

- Reliability and robustness.

- Reasonable cost.

General specifications of the machine can be performance specifications or/and size specifications, a list of general specifications is listed as follows:

- Motor rotating torque.

- Power.

- Speed.

- Efficiency.

- Stator outer diameter, stack length.

5.5.2 Initial sizing and pre-design decisions

After the specifications of the motor were defined, the designer must come with some decisions, those decisions are made initially to simplify the analytical design but also to prevent or satisfy some other specifications such as efficiency, saturations.. etc.

The following equation is used to compute the motor torque (Hendershot & Miller, 1994):

$$T = \frac{\pi}{4}.\sqrt{2}.K_w.A.B_g.D_A{}^2.L_{stK} \qquad \text{5-8}$$

$$T = \frac{\pi}{4}.TRV.D_A{}^2.L_{stK} \qquad \text{5-9}$$

Where:

- TRV: torque per unit rotor volume.

- D_A: Air gap diameter.

- L_{stK}: stack length.

The previous equation shows that the torque is related to the rotor volume, here the torque per unit rotor volume is the produced torque from a given rotor volume. The TRV value depends also on the application of the machine, according to the application (Miller, 1989) provides the designer with some typical TRV values.

5.5.3 Motor control

A commercial regulation and control equipment SEVCON Gen4 Size2 was selected, with the following characteristics:

Model	Size 2
Nominal Battery Voltage	36 - 48 VDC
Max. Operating voltage	69.9 VDC
Min. Operating voltage	19.3 VDC
Peak Current (2min)	275 A
Boost current (10sec)	330 A
Cont. Current (60min)	110

table 8 SEVCON Gen4 characteristics.

Figure 21 SEVCON Gen4 Size2

To determine the position/speed: an incremental or absolute encoder is used, which can be defined as an optoelectronic device that provides electrical signals, pulse train, from which it is possible to determine the angular position of the input shaft. For the designed motor, an incremental encoder would be used which would be attached to the shaft.

Figure 22 Encoder

The Hall effect sensor is formed of 3 out of phase $\frac{120^{o}}{p}$ Hall sensors, these sensors can be centred on the axis of the stator teeth. With this phase shift and through the Hall effect they give the position of the rotor.

Figure 23 Sensor Hall

Gen4 is used to control the power of PMSM motors in electric vehicles, here a 4 quadrant control of speed and torque is applied (driving and braking torque in the forward and reverse directions).

5.5.4 Number of poles and slots selection

The selection of the number of poles and slots is a very important process since it affects the performance of the machine and that's because of the dependence of some properties on this configuration such as torque ripple, a good selection of poles and slots numbers can avoid noises and vibrations and can cause the reduction of torque ripple/cogging torque.

The ratio between the number of poles and the number of slots is a very important factor. According to (Gieras & Wing, 2002) the higher this ratio the better, since it's inversely proportional to the cogging torque value. While (Hendershot & Miller, 1994), set groups for poles and slots number combinations suitable for three phase PMSM motors.

There is no specific rule to select the number of poles, but the relation between the machine speed and the number of poles can be a start point to define the number of poles (Chau, 2015):

$$n = \frac{60f}{p} \qquad \text{5-10}$$

Where:

- f: frequency

- p: pole-pairs

The power can be calculated as follows (Hanselman, 1994):

$$P = T\omega \qquad \text{5-11}$$

Where:

- ω: is the rotational speed, and can be obtained as follows:

$$\omega = \frac{60n}{2\pi} \qquad \text{5-12}$$

From the previous equation, it can be seen that for applications of high-speed a small number of poles have to be chosen and for low-speed application higher number can be chosen.

(Hanselman, 1994) set some assumptions to simplify this process and to reach a desirable number of poles and slots, the assumption considered in this thesis are:

- All slots are filled, which mean that the slots number is a multiple of the phase number.

- The number of slots per pole per phase (q) is assumed to be less than or equal to two.

- The number of slots can be calculated according to the following equation (Pyrhonen, et al., 2008):

$$Q = q.m.2p \qquad \text{5-13}$$

Where:

- q: number of slots per pole per phase.

- m: phase number

- p: pole-pairs

5.5.5 Air gap dimensions

The stator and the rotor are magnetically coupled, therefore there is an air gap between them. When the machine works a magnetic field is set up and links both stator and rotor, here not all of the magnetic field is utilized and part of it leaks through the air gap (leakage flux).

The leakage flux is not useful it actually causes power losses since it is not linked to the stator and the rotor, the air gap length is inversely proportional to the leakage flux, therefore the air gap length must be maintained at its minimum possible to assure the separation between rotor and stator and to provide the required mechanical balance of the machine.

As mentioned before, to reach the maximum value of flux per pole and to reduce the dispersion of magnetic flux, a small air gap value is desirable, (Hendershot & Miller, 1994) set the air gap value according to the power level:

- 0.13< Lg < 0.25, for low power machines.

- 0.38< Lg. <0.51, for medium power machines.

- 0.64< Lg <0.89, for high power machines.

After the selection of the air gap length along with the PM material, the flux and flux density of the air gap can be calculated (Hanselman, 2006):

$$B_g = \frac{K_1.B_r}{1 + K_r.\frac{L_g}{L_M}.\mu_r} \qquad \text{5-14}$$

Where:

- K_1=Leakage factor, typically $0.9 \leq K_1 < 1.0$.

- K_r=Reluctance factor, typically $1.0 < K_r \leq 1.2$.

- B_r= Magnetic remanence.

- μ_r= Permeability of the magnet, which can be calculated as follows:

$$\mu_r = \frac{B_r}{\mu_0 H_C} \qquad \text{5-15}$$

Where:

- μ_0: Relative permeability of vacuum with s value of $4\pi \times 10^{-7}$ H/m.

- H_C: Coercivity.

- L_M=Magnet Length, according to (Hendershot & Miller, 1994), this can be calculated in function of the permeance coefficient PC:

$$PC = \frac{L_M}{L_g} \qquad \text{5-16}$$

Usual values for PC are between 5 and 15, and according to (Hendershot & Miller, 1994), the first estimate for magnets of high coercive force (rare earth magnets) is to take the value of this coefficient as 10.

And the Air gap flux can be calculated using the following equation:

$$\emptyset_g = \frac{\sqrt{2}.B_g.D_A.L_{stK}}{p} \qquad 5\text{-}17$$

5.5.6 Winding and stator sizing

To start with the winding sizing, the first selection is whether the winding is a single or double layer, the decision can be made taking into account the comparison study between both types which were made in chapter 2 and also assumptions made in (Hanselman, 2006).
Once the layer is selected, the number of coils can be calculated as follows:

$$Nc = \frac{Q.Layers}{2} \qquad 5\text{-}18$$

Which gives a number of coils per pole and phase:

$$n_c = \frac{Nc}{2p.m} \qquad 5\text{-}19$$

The number of turns can be calculated as following (Pyrhonen, et al., 2008):

$$E = \sqrt{2}\pi f \emptyset_g k_w N \qquad 5\text{-}20$$

Where:
- E: Induced phase voltage.
- k_w: Winding factor.
- N: Turns number.

The selected number of turns must be an integer and a multiple of 3 (phase number).

Now the stator dimensions can be defined, the slots, as well as the teeth dimension, must be defined, according to (Chau, 2015), those dimensions are related to the pole pitch and the slot pitch and can be calculated as follows:

- *Pole pitch:* $\tau_p = \frac{D_A \pi}{2p}$ 5-21

- *Slot pitch:* $\tau_s = \frac{\tau_p}{Q/2p}$ 5-22

Now, the slot width and the tooth can be calculated in function of the maximum flux density in the tooth, where (Pyrhonen, et al., 2008) set the permitted value in function of the machine type:
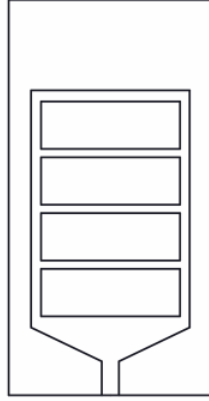
Figure 24 Slot model (Bianchini, et al., 2020)

$$w_t = \frac{\tau_s}{k_{Fe} B_{max,tooth}} B_g \qquad\qquad 5\text{-}23$$

Where:

- $B_{max,tooth}$: Maximum flux density in the tooth.
- k_{Fe}: Space factor.

$$w_s = \tau_s - w_t$$

The slot area can be obtained:

$$A_s = \frac{n_{c/slots} a_c}{F_F} \qquad\qquad 5\text{-}24$$

Where:

- a_c: Conductor area.
- $n_{c/slots}$: Number of conductors per slot.
- F_F: Filling Factor.

The number of conductors area can be calculated as follows:

$$a_c = \frac{I}{\delta} \qquad\qquad 5\text{-}25$$

Where:

- δ: Maximum flux density.

$$I = \frac{P}{3.E.\eta.\cos\theta} \qquad\qquad 5\text{-}26$$

And the number of conductors per slot:

$$n_{c/slots} = \frac{N}{Nc/3}.Layers \qquad\qquad 5\text{-}27$$

Since the winding is hairpin and the slot is rectangular, the slot height can be calculated as follows:

$$h_s = \frac{A_s}{w_s} \qquad\qquad 5\text{-}28$$

Finally, the stator yoke highest can be calculated as follows (Pyrhonen, et al., 2008):

$$h_{cy} = \frac{\emptyset_g}{2k_{Fe}B_{max,yoke}L_{STK}}$$ 5-29

Where:

- $B_{max,yoke}$: Maximum flux density in the stator yoke.

5.5.7 Rotor sizing

The selected rotor geometry of PMSM was the V-shape, this geometry is one of the most complicated shapes of PMSM, but (Lin, 2017)provides the necessary equations to define the magnet slot geometry.
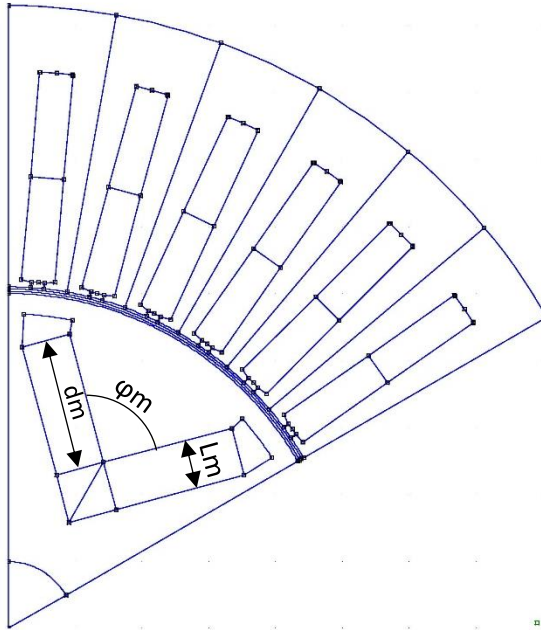
Figure 25 The angle span of the magnet φ_m is defined by:

$$\varphi_m = \frac{2\pi}{2p}\alpha_{pm}$$ 5-30

Where:

- α_{pm}: The angular fraction of the magnet pair (0 < α_{pm} < 1).

While the depth of the permanent magnet d_m is defined by :

$$d_m = \alpha_{dm}L_m$$ 5-31

Where:

α_{dm}: is the aspect ratio of the permanent magnet.

5.6 **Numerical model (FEM Analysis)**

Numerical methods are used to solve complicated problems which include differential and integral equations. Many software is designed to solve numerical problems, in the beginning, software was very slow and not accurate but now the designer can find a variety of software which can be used, some of them are paid and others are free.

The most widely used method is the finite element method (FEM), which can be used to solve 2D or 3D problems, and it can solve magnetically, electrostatics, heat flow and current flow problems. It's based on dividing the volume or domain in which the equation is valid, into smaller volumes or domains. Within each element, a simple polynomial is used to approximate the solution. In other words, the discretization transforms the partial differential equations into numerous nonlinear algebraic equations.

The FEM is a highly used resource in engineering and physics, and its applications are multiple. By applying this technique correctly, it is possible to carry out numerical calculations of complicated geometries with great precision.

Finite elements are connected by nodes, points in space where the equations of the problem are solved. Interpolating between the values found for each node, the value of the equations in the finite elements delimited by each node is defined. The set of nodes and finite elements make up the analysis mesh. The more discretized (smaller elements) the more exact mesh will be the solution.

It's important to mention that in electric machines as PMSM the air gap is considered one of the most important design parameters since most of the magnetic energy is stored in it and important torque and other calculation are related to the air gap, therefore the mesh size in the air gap must be sufficiently dense.

For this thesis FEMM software was selected to perform the simulation and obtain the results, a 2D section of the machine was simulated, first of all, the problem was defined as well as the materials for each region, then the mesh size and the boundaries of the machine after all the results were obtained directly from the FEMM and with the help of Lua scripting language.

6 Results

In this chapter the results of the machine design will be presented, after the machine design process in the analytical model simulations were carried out to validate the machine behaviour.

6.1 Analytical model

This chapter shows the results from the analytical model, the machine dimensions and machine properties are shown.

6.1.1 Specifications and machine characteristics

The objective of the designed machine was to build a small motor which is suitable to be assembled manually, which limit its specifications to size specifications, in the following table the selected parameters of the machine, parameters were selected taking into account firstly the size specification when compared to other machines which have a similar size:

table 9 Specifications of the machine.

Parameters	Symbol	Value	Unit
Air gap diameter	D_A	100	mm
Stack length	L_{STK}	80	mm
speed	n	1910	r.p.m

6.1.2 Initial design sizing and pre-design decisions

The pre-design decisions assure a good design, for example, the efficiency was set to 99% so the calculated parameters chosen for the motor will be based on this value, other decisions were taken by a comparison study of similar motors and finally, the listed books in the literature review have assumptions of PMSM design process and were taken into account in this thesis.

table 10 Pre-design decisions

Parameters	Symbol	Value	Unit
Torque per unit rotor volume	TRV	35000	Nm/m^3
Air gap length	L_g	1	mm
Number of slots per pole phase	q	2	-
Leakage factor	K_1	0.9	-
Winding factor	K_W	0.9659	-
Space Factor	K_{Fe}	0.97	-
Filling factor	FF	0 .6	-
Maximum tooth flux density	$B_{max, tooth}$	1.8	Tesla
Maximum yoke flux density	$B_{max, yoke}$	1.5	Tesla
Maximum current density	δ	3	A/mm^2
$\cos\theta$	-	1	-
effeciency	η	0.99	-

6.1.3 Number of poles and slots

The number of poles and slots was selected using the set tables of the number of poles and number of slots combination in (Hendershot & Miller, 1994)

Parameters	Symbol	Value	Unit
Poles number	p	6	-
Slots number	Q	36	-

table 11 Number of poles and slots.

6.1.4 Air gap dimensions

Parameters	Symbol	Value	Unit
Air gap flux density	B_g	1.13	Tesla
Air gap flux	$\emptyset_g$	$3.95*10^{-3}$	Wb
Relative permeability	μ_r	1.08	N/A^2

table 12 Air gap dimensions

6.1.5 Winding and stator sizing

table 13 Stator parameters

Parameters	Symbol	Value	Unit
Pole pitch	τ_p	52.36	mm
Slot pitch	τ_s	8.72	mm
Tooth width	w_t	5	mm
Slot width	w_s	3.72	mm
Slot highest	h_s	30	mm
Slot area	A_s	110	mm^2
Yoke highest	h_{cy}	22	mm

table 14 Winding parameters

Parameters	Symbol	Value	Unit
Number of Coils	N_c	36	-
Number of turns	N	18	-
Number of conductors per slot	$n_{c/slots}$	4	-
Conductor area	a_c	16	mm²

6.1.6 Rotor sizing

Parameters	Symbol	Value	Unit
The angular fraction of the magnet pair	α_{dm}	2	-
The aspect ratio of the permanent magnet	α_{pm}	0.5	-
Magnet length	L_M	10	mm
Angle span	φ_m	30	degree
Magnet depth	d_m	20	

table 15 Rotor parameters.

6.1.7 Machine specifications

table 16 Final machine specifications

Parameters	Symbol	Value	Unit
Torque	T	21	N.m
speed	n	1910	r.p.m
Frecuency	f	95.5	Hz
Power	P	4.2	Kw
Current	I	65	A
Phase voltage	E	21.6	V

6.2 Numerical model (FEM Analysis)

As mentioned in chapter 2; The objective of the finite element analysis is to verify the model designed in the analytical method, this process is carried out by an own-developed finite element method magnetics package (FEMM) software. FEMM software allows the users to solve magnetics, electrostatic and thermal analysis. The Lua scripting language is used to obtain different results such as the inductances, torque, back EMF, and losses.

6.2.1 Machine geometry and Material setting

The start point of the fem analysis is to drow the 2d model of the machine, the 2d section was drawn and the imported to the software.
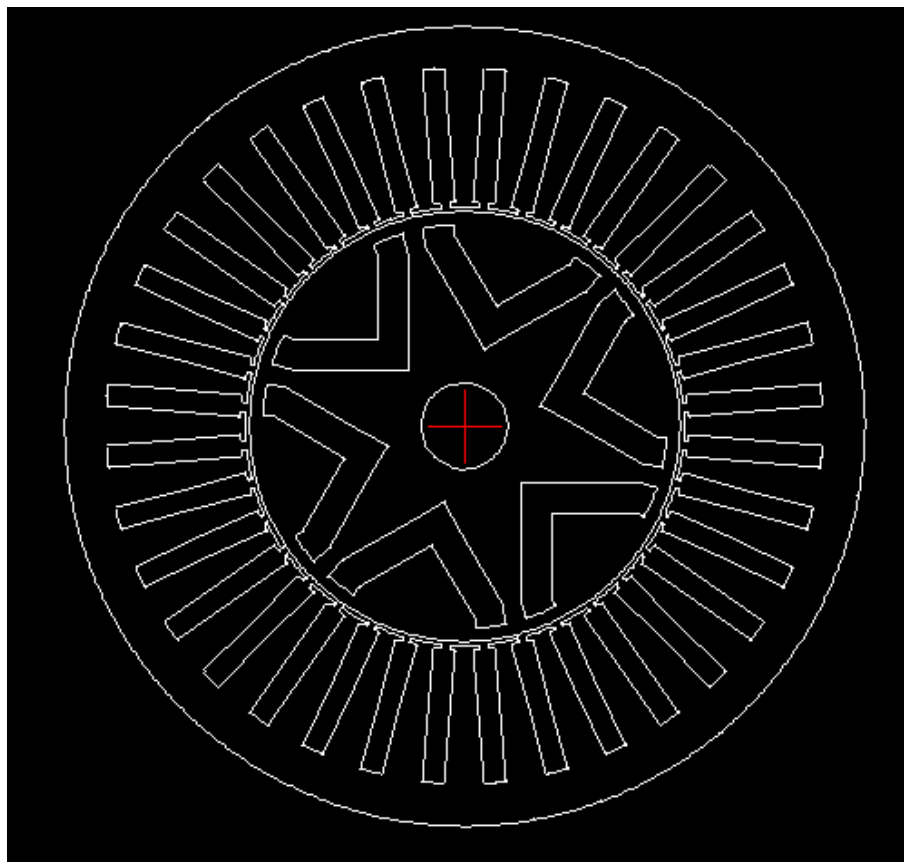
Figure 26 The motor design in AutoCAD.

After the CAD drawing is imported to FEMM software, the problem properties must be defined, the material and their properties for each region of the motor have to be set, and the boundary properties have to be added The materials can be set from FEMM material library or added to the library in case of new material.

The selected material and their properties were discussed in chapter 4, figure() shows the motor with the materials assigned to each region. it's important to note that when the magnet material is set, the magnetization direction for each magnet region must be defined. And when it comes to the winding the copper was assigned but also the number of turns and the circuits/phases(A, B, C) were assigned also.
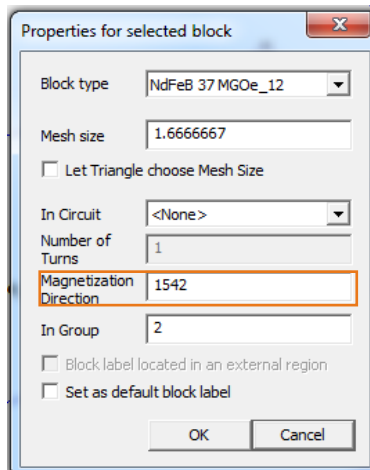
Figure 28 Selection of circuits and number of turns.
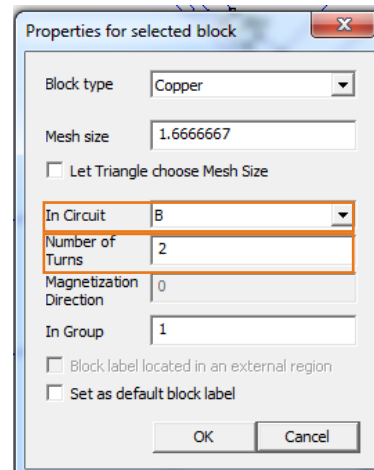
Figure 27 Magnetization direction in FEMM.
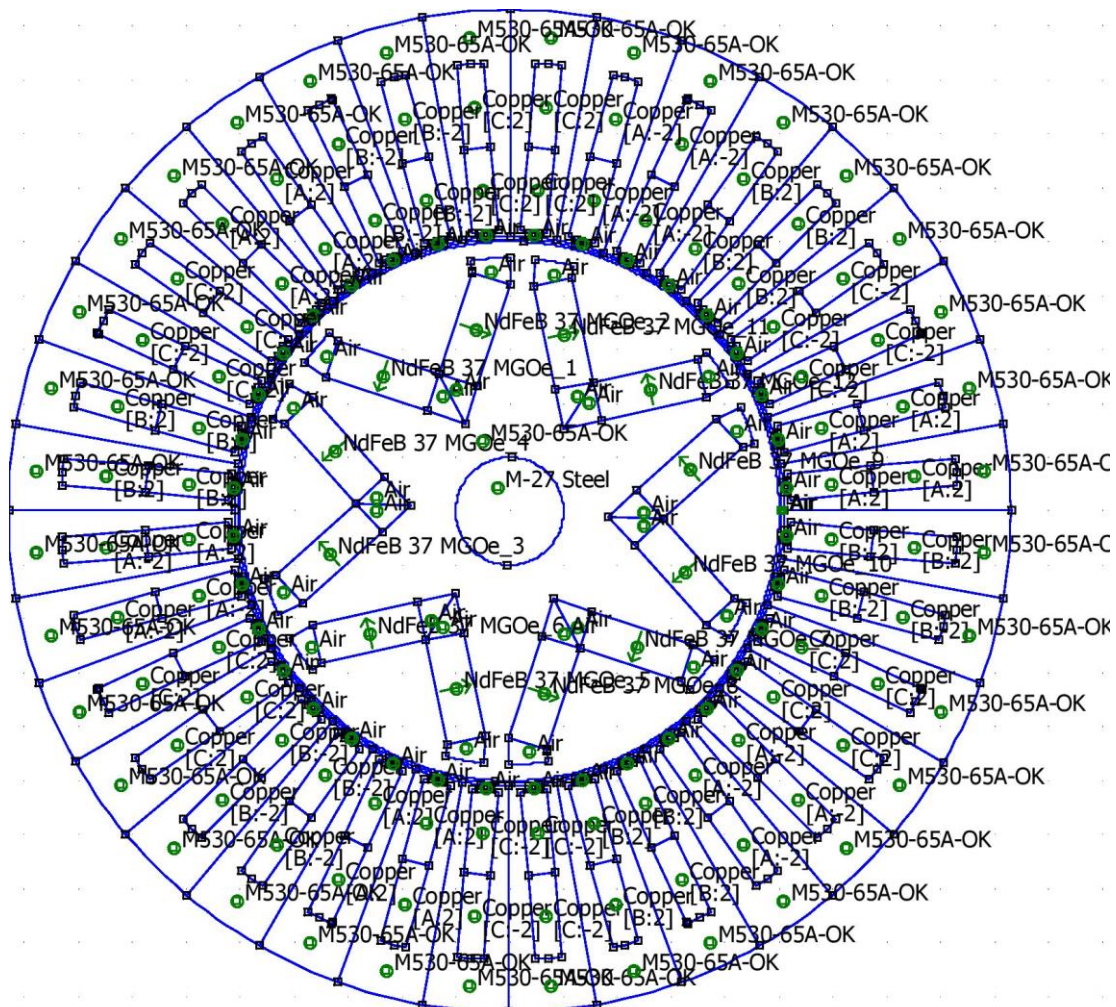
Figure 29 Materials assigned for each region of the motor.

6.2.2 Accuracy parameters

Mesh size

The accuracy of the calculation depends on the mesh size therefore it's important to set a suitable size of it since the big mesh size leads to poor calculations but the very small mesh leads to a long time of calculations. in this type of electric motor, the air gap, and the magnets affect the final results more than the other parts of the motor therefore a smaller mesh size was assigned for these regions.
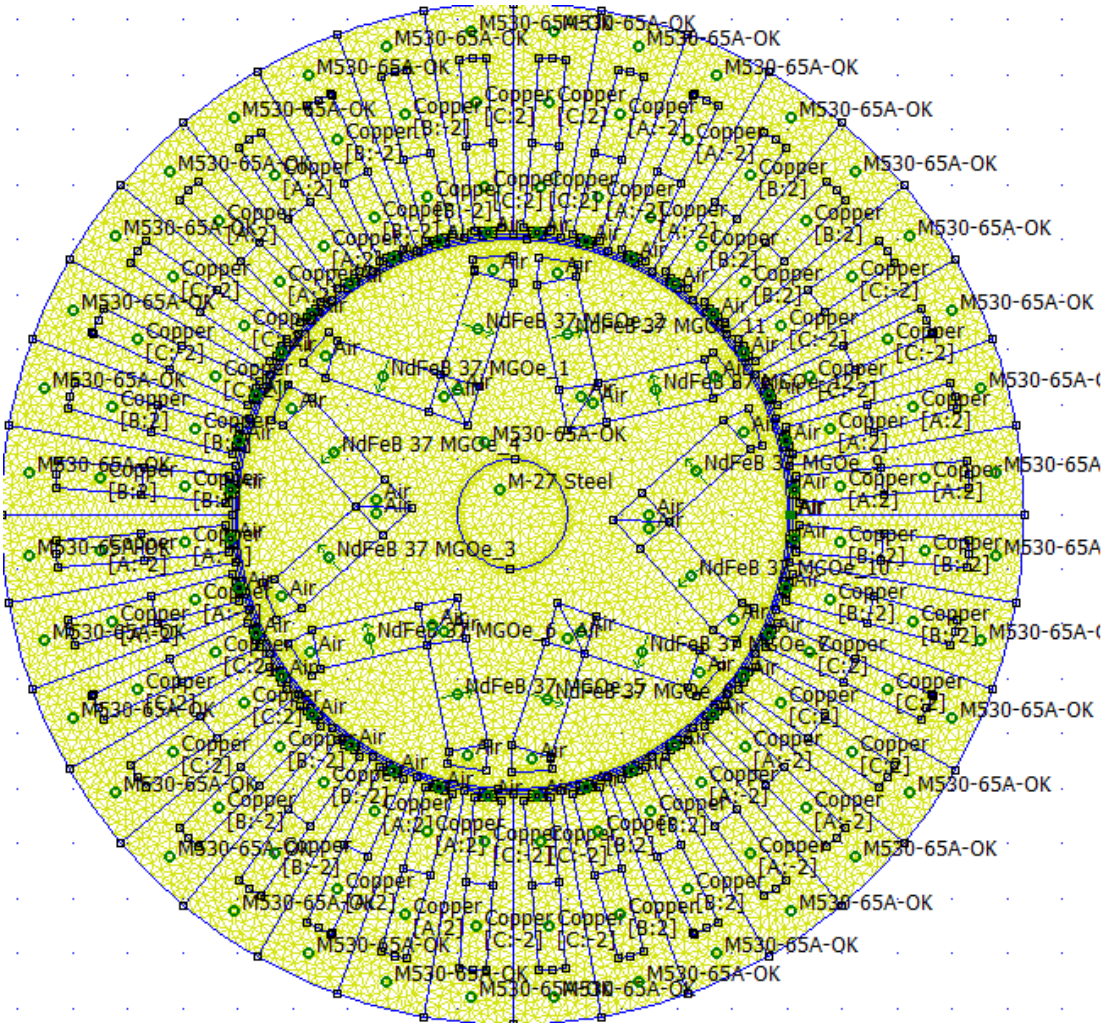
Figure 30 Created mesh
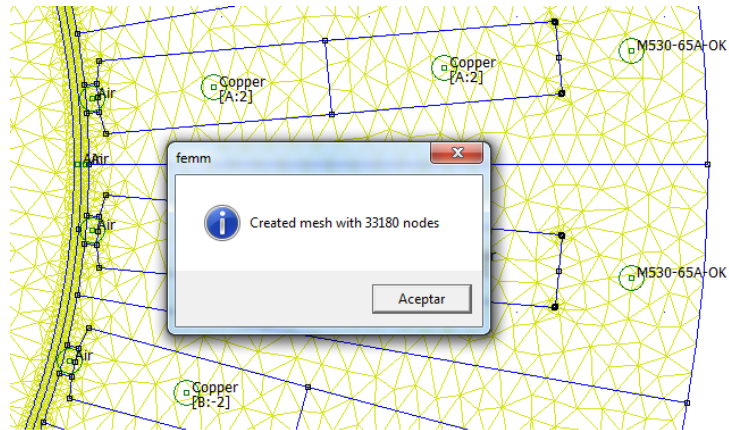
Figure 31 Created mesh with 33180 nodes.

6.2.3 Simulations results

A. Flux density and magnetic field lines
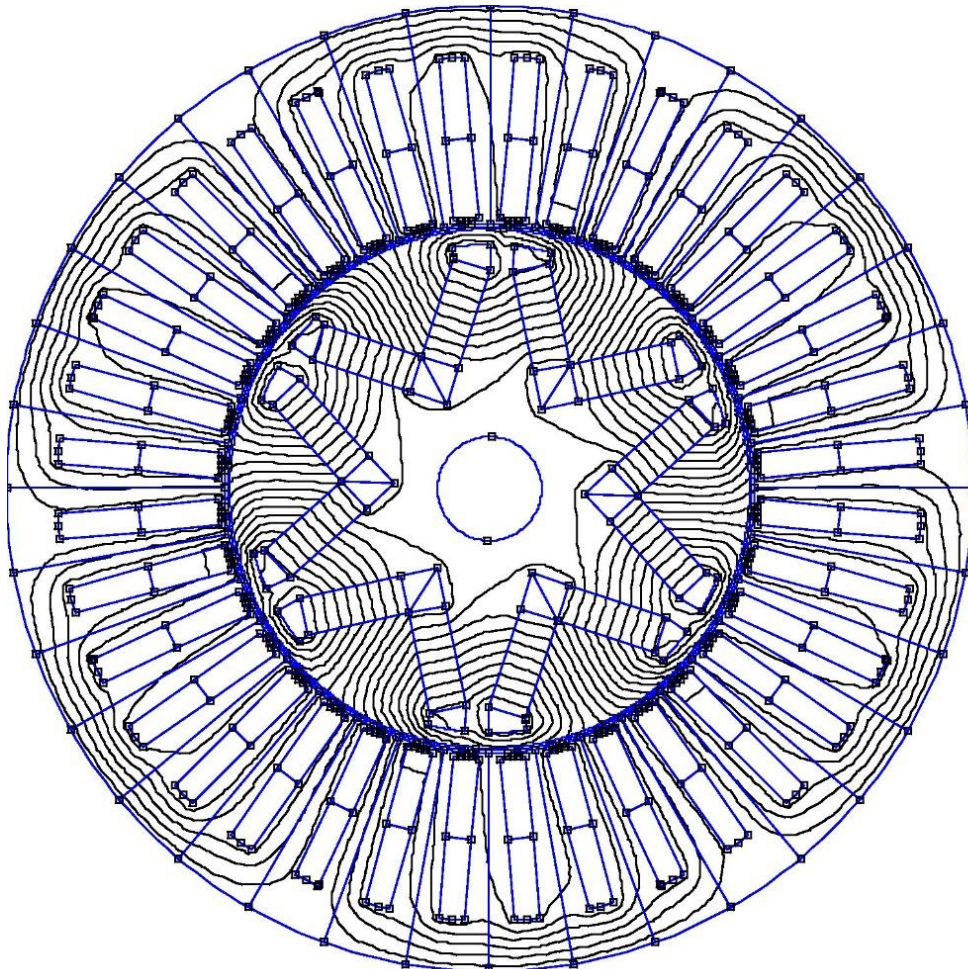
Figure 32 No-load distribution of magnetic field lines

The previous figure shows the magnetic field lines of the machine poles, there are 6 poles and it can be seen that there are 6 magnetic field lines regions.

The first analysis of the machine was done in a no-load case and no three-phase current in the stator winding, the following figure shows the no-load magnetic field which is created only by the rotor's permanent magnets. FEMM software shows the flux density in each region by colours, the darker colours express high flux density. The regions near the permanent magnet are highly saturated as can be seen in the metal sheet near the magnets.

| 2.122e+000 : >2.234e+000 |
| 2.011e+000 : 2.122e+000 |
| 1.899e+000 : 2.011e+000 |
| 1.787e+000 : 1.899e+000 |
| 1.676e+000 : 1.787e+000 |
| 1.564e+000 : 1.676e+000 |
| 1.452e+000 : 1.564e+000 |
| 1.340e+000 : 1.452e+000 |
| 1.229e+000 : 1.340e+000 |
| 1.117e+000 : 1.229e+000 |
| 1.005e+000 : 1.117e+000 |
| 8.937e-001 : 1.005e+000 |
| 7.820e-001 : 8.937e-001 |
| 6.703e-001 : 7.820e-001 |
| 5.586e-001 : 6.703e-001 |
| 4.469e-001 : 5.586e-001 |
| 3.352e-001 : 4.469e-001 |
| 2.235e-001 : 3.352e-001 |
| 1.118e-001 : 2.235e-001 |
| <1.130e-004 : 1.118e-001 |

Density Plot: |B|, Tesla

Figure 33 No-load distribution of flux density

The following figure shows the Air gap flux density obtained from FEMM, it can be observed that the value is near to 1 Tesla which is very close to the value obtained from the analytical model (1.14T).
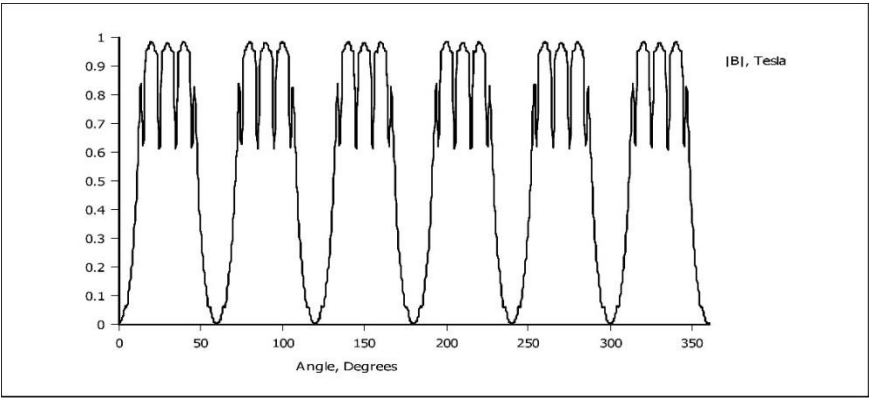
Figure 34 Air gap flux density

Rapid variations of the magnetic field are mainly due to the presence of teeth and slots of the stator area.

B. Rotating torque

The rotating torque is developed when the motor rotates at nominal current and nominal speed, the simulation is carried out by rotating the rotor with the nominal current in each phase of the stator winding, while FEMM works with a three-phase balanced current system and peak current values.
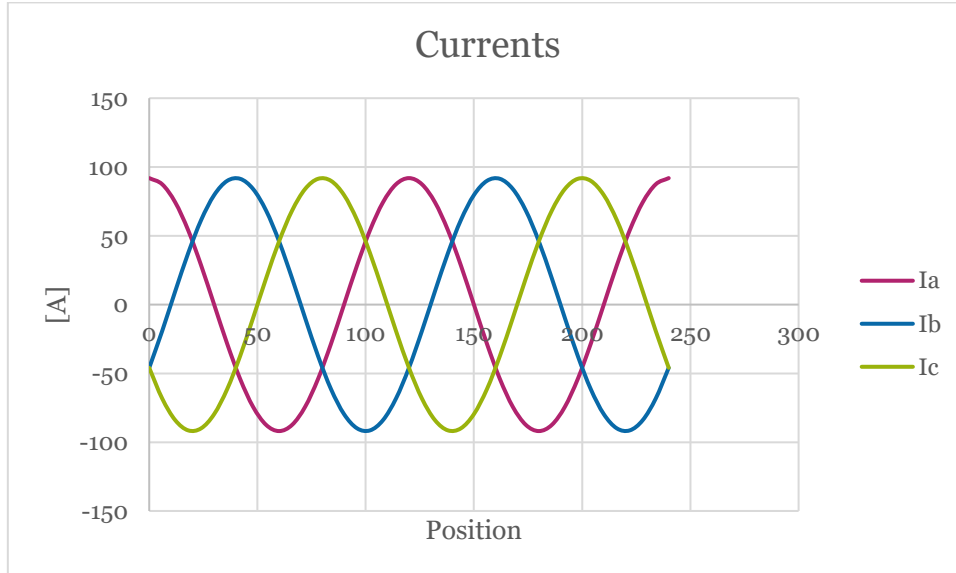
Figure 35 Phase currents
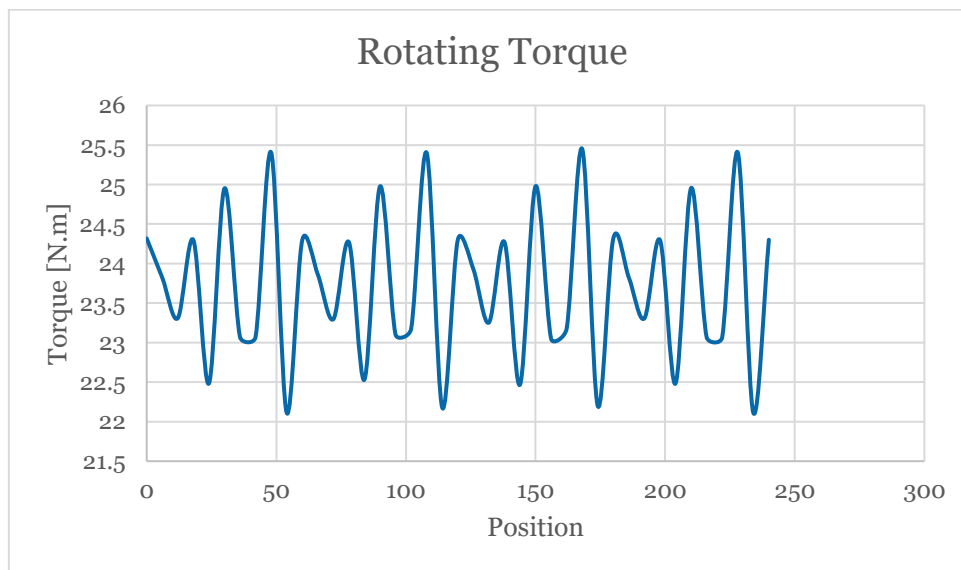
Figure 36 Rotating torque

It can be observed that the maximum torque developed by the motor at nominal current is:

$$T_{max} = 25,5 \ N.m$$

Which gives:

$$P_{max} = T_{max} * \omega_n = 5100 \ W$$

C. Cogging torque

Cogging torque is a detent torque that occurs in PMSMs due to the interaction between permanent magnets and the stator teeth, as was discussed in chapter 2.

To obtain the cogging torque, a simulation was carried out only with the PMs, the rotor will be rotated from 0° to 120° (mechanical angle) and the data is obtained for each position of the rotor.
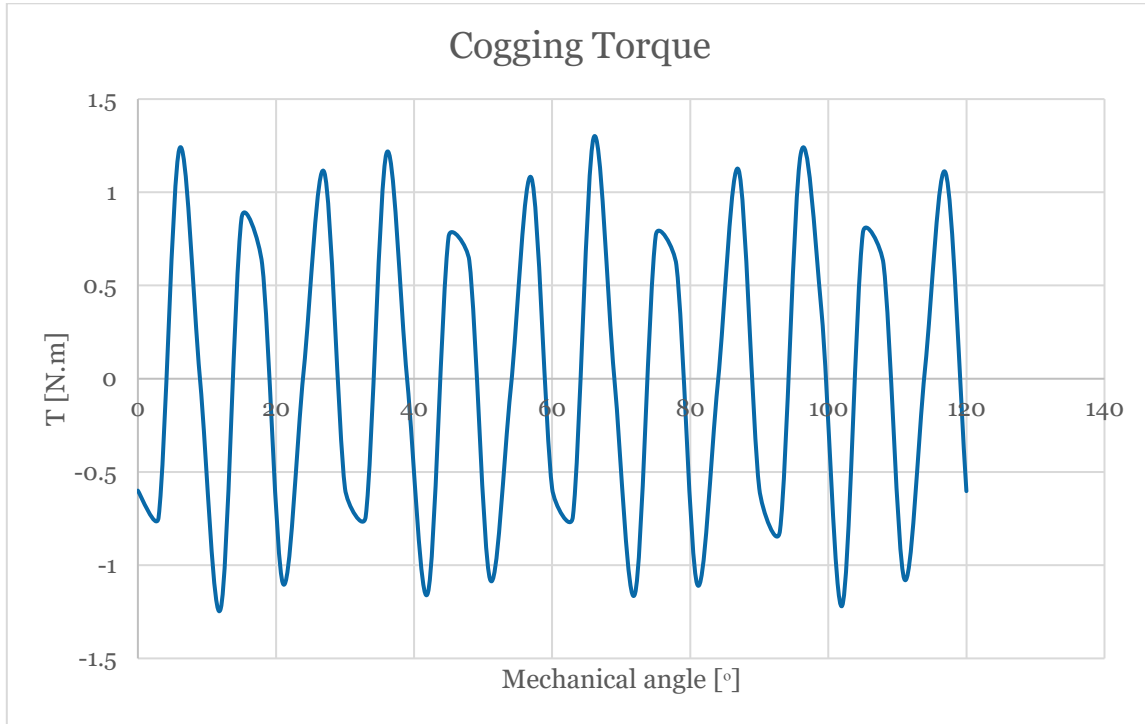
Figure 37 Cogging torque

The maximum value of cogging torque is 1.29 N.m, and the mean value is 0.747 N.m. therefore the percentage of cogging torque is:

$$Cogging(\%) = \frac{mean\ cogging}{T_{max}} * 100 = 2.92\% \qquad 6\text{-}1$$

Which gives a percentage of ripple torque around 14%.those values according to (K.T.Chau, 2015) are very acceptable for EV propulsion applications. even though it's important to note that the ripple torque is affected by many factors, as mentioned in chapter 2, a lower value of ripple torque can be achieved through the machine geometry optimization, since it's greatly affected by the rotor and magnet geometry, which can be considered as a future work of this thesis.

D. Inductances

To obtain the machine inductances a simulation was carried out to calculate the magnetic field energy of the air gap, the free spaces, the permanent magnets, and of the coils, once the magnetic field energy is obtained the following equations are used to determine Ld, Lq values:

$$W = \frac{m}{2} * L_m * I^2{}_m \qquad 6\text{-}2$$

In (d-q) frame, the minimum value of the magnetic field energy is produced by the d axis and the maximum value is produced by the q-axis, the inductances can be calculated through:

$$L_d = \frac{W_{min}}{\frac{m}{2} * I_n^{\,2}} \qquad \text{6-3}$$

$$L_q = \frac{W_{max}}{\frac{m}{2} * I_n^{\,2}} \qquad \text{6-4}$$
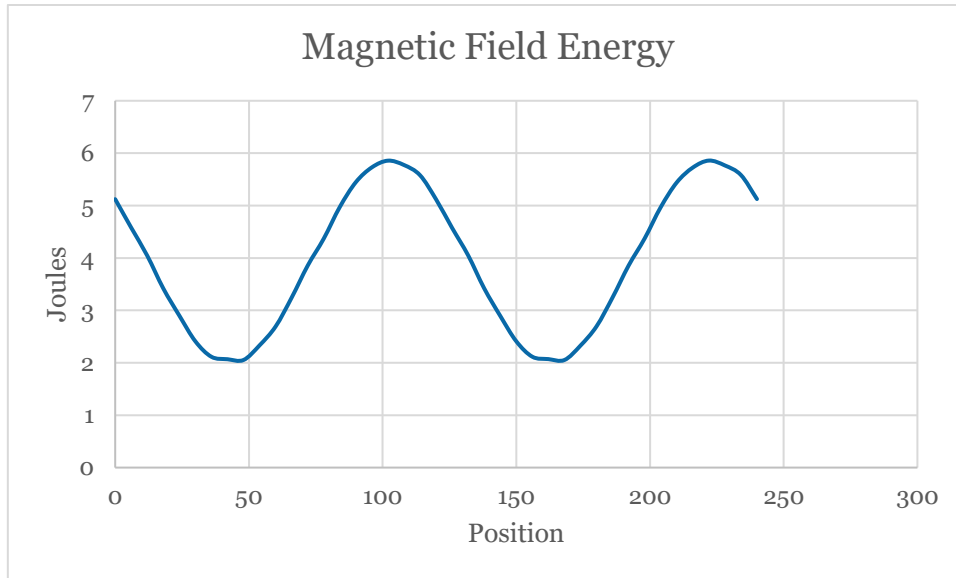
Figure 38 Magnetic field energy

Magnetic field energy of the air gap, the free spaces, the permanent magnets, and of the coils

Which gives:

Ld = 3.239 * 10^{-4} H

Lq = 9.245 * 10^{-4} H

E. EMF determination

The back electromotive force is produced by the permanent magnet so to obtain this value a simulation with the no-load condition is carried out, which means that the current through the winding coils is set to 0 and the fluxes created by the permanent magnets is obtained, once the fluxes values of the three phases are obtained the following equation is used to obtain the EMF of the three phases:

$$e = \frac{\varnothing_2 - \varnothing_1}{\theta_2 - \theta_1} * \omega \qquad \text{6-5}$$

Where:

$$\omega = \frac{2 * \pi}{60} * n \qquad \text{6-6}$$
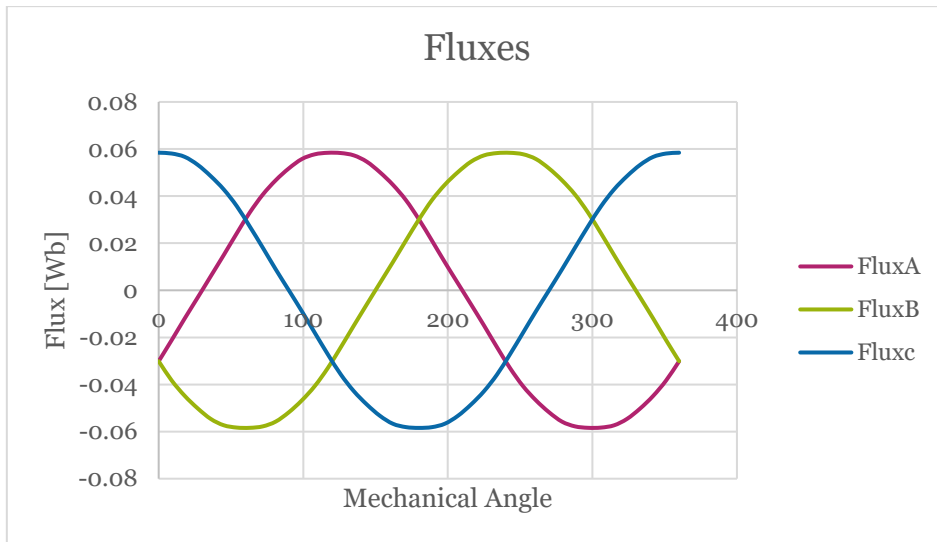
Figure 39 Phase fluxes
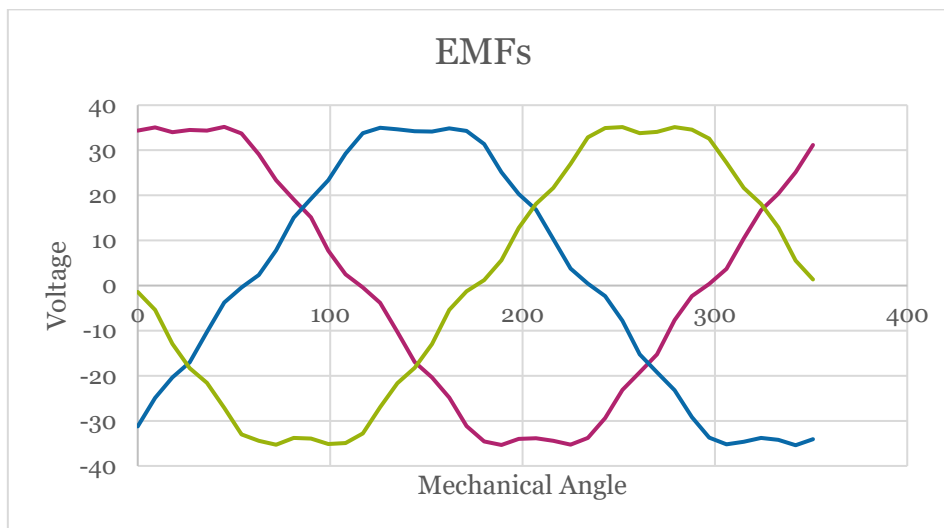
Figure 40 Induced EMF

The maximum value of EMF is 35 V.

F. Losses

1) Iron losses

Iron losses are caused by hysteresis losses and Foucault currents, to obtain them, the simulation was carried out using the analytical equation from Bertotti:

$$P_{fe} = \frac{1}{\gamma}\left(K_h.f.B^2 + K_c.f^2.B^2 + K_a.\sqrt{f^3 B^3}\right) \qquad 6\text{-}7$$

Where:

- B: Induction
- γ: Specific iron density
- K_h, K_c, K_a: Coefficients of the metal sheet
- f: frequency

Figure 41 Iron Losses

Iron losses = 25 W.

2) Copper losses

Femm provides the users with the copper losses directly from the result window post-processor.
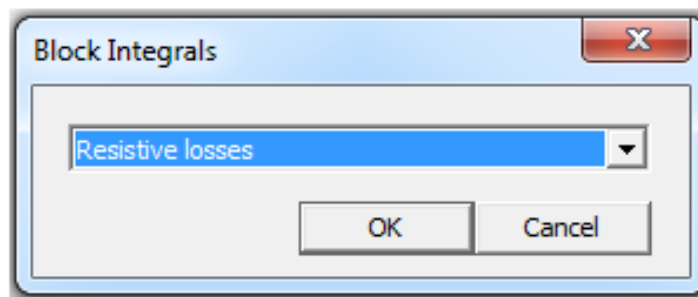
Figure 42 Resistive Losses in FEMM
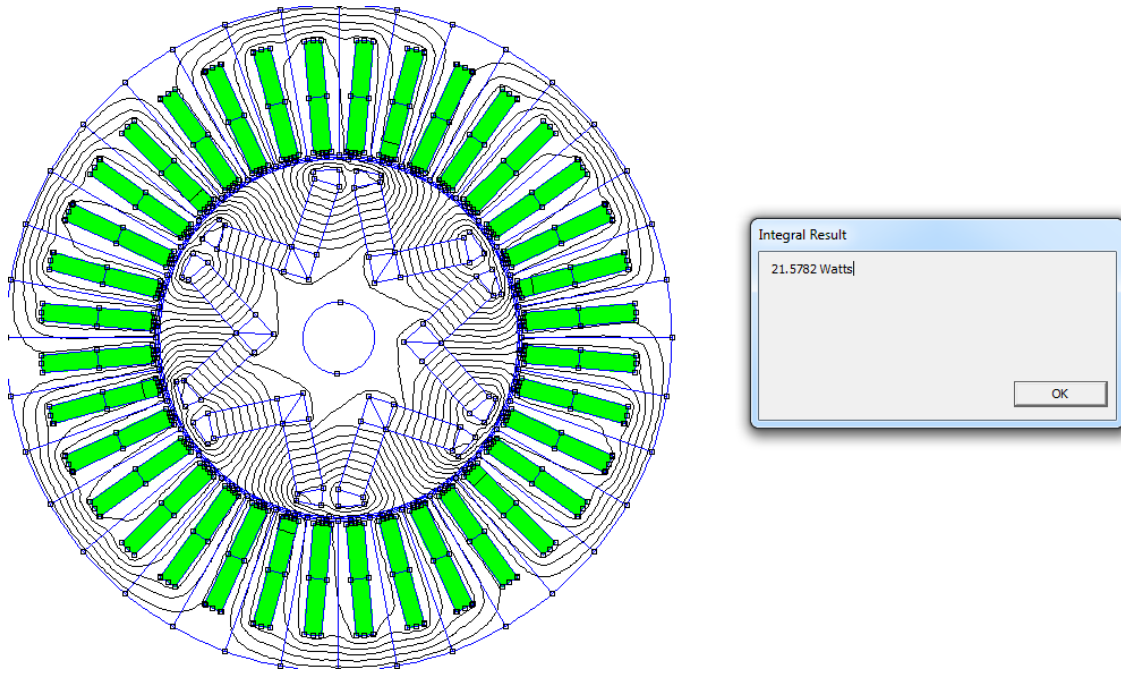
Figure 43 Resistive Losses in FEMM

Copper losses = 22 W

By using Hairpin winding the copper losses are minimized and the efficiency maximized.

G. Efficiency

The following equation is used to calculate the efficiency:

$$\eta = \frac{P - Total\ Losses}{P} * 100 = 98.88\% \qquad 6\text{-}8$$

Where:

P: Motor Power

The efficiency value is high but this value will be reduced in practice due to mechanical elements.

7 Prototype assembly and test

7.1 Prototype assembly

The prototype assembly consists of different parts and different technologies were used to reach the final motor body, once the design was validated, the lamination cutting and stacking process were selected.

After the motor cores are formed, the winding process can be performed which consists of inserting the hairpin wires into the stator slots, finally, the permanent magnets are inserted into the rotor slots and the final assembly is performed.

It's important to note that the disassembly of the motor pieces must be possible since this prototype is designed for the manufacturing lab and the students will perform the assembly and disassembly each time they run the lab.

In this chapter, the selected methods and the results are described as well as the assembly instructions for each phase.

7.1.1 Cutting process

The laser cutting method was chosen to cut the laminations of the core of the designed motor, the process was performed by the University of Skovde laser cutter, 160 (M530-65A)sheets with 0.5 mm thickness were cut to form an 80 mm stack of motor core, the following figure shows a cut sheet of the rotor and the stator
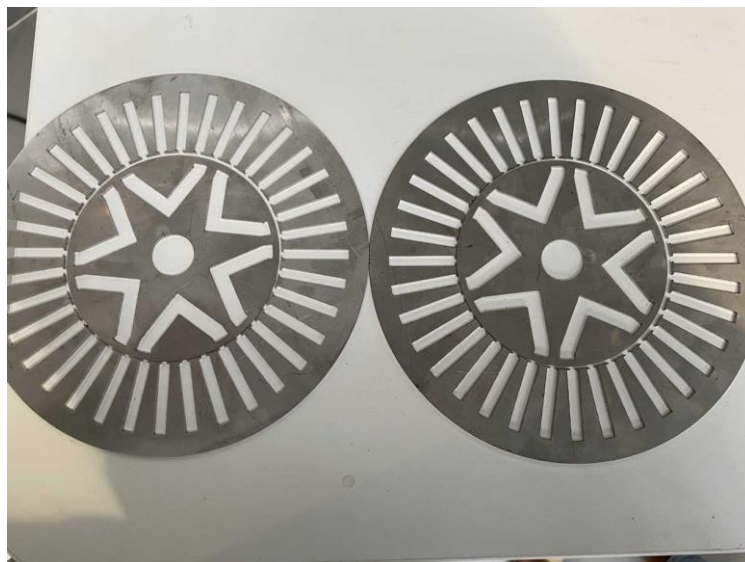
Figure 44 Lamination sheets

Assembly instructions

1- Prepare the motor 2D drawing and upload it to the laser cutter software.

2- Set the dimensions of the 2D design. (it's important to match the selected dimensions with the used material size).

3- Select the used material in the laser cutter material list.

4- Place the material in the centre of the laser cutter.

5- Clean the laser cutter lens with rubbing alcohol.

6- Set the lens highest and Turn on the fume extractor.

7- Press the cut bottom.

7.1.2 Stacking process

It's very important to produce a stack of even quality since the misalignment between the sheets causes difficulties in the assembly of the stator in the housing which causes undesirable contact between them that leads to low heat transfer and an increasing of the motor temperature.

In the electric motor manufacturing line, auto lamination stacking and welding machines are used to perform this phase of the assembly process, but since this prototype is designed for teaching purpose the stacking process will be performed by hand.

The welding method was used to perform the laminations of the core stacking, according to (Pyrhonen, et al., 2008) the stack must be straightened then pressed into the final length.

The chosen method in this thesis to straighten the stack is to use guides in the slots of the stator and the rotor, then. the stack is clamped by Seger rings.

Figure 45 Stacking guides (Sarrico, 2017)

Welding is applied to the outer surface of the stator stack, to avoid the increase of the stator outer diameter small cuts along the motor length are made in the surface of the cores and then the stack is welded at these cuts

7.1.3 Winding process

Before the winding process is performed, it's important to define the winding parameters as mentioned in the following table:

Parameters	Symbol	Value	Unit
Number of Coils	N_c	36	-
Number of turns	N	18	-
Number of conductors per slot	$n_{c/slots}$	3	-
Conductor area	a_c	22	mm²

table 17 winding parameters

- Coil span = Q/p = 6

Hairpin winding consists of various steps which are defined as follows:

1- Shaping.

2- Assembly.

3- Twisting.

4- Welding.
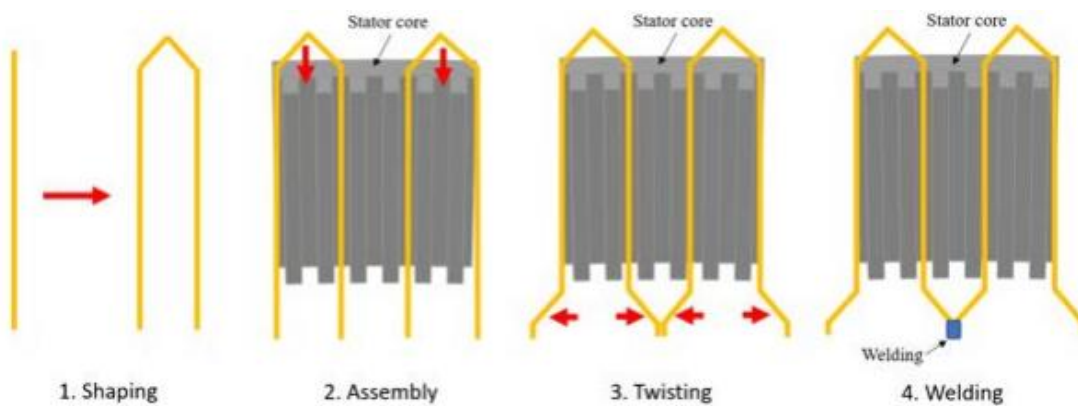
Figure 46 Hairpin winding assembly (Limited, 2021)

Assembly instructions

1- A copper rectangular wire of 22 mm^2 is shaped into hairpin form; tacking into the coil span (6 slots).

2- Prepare the stator slots by inserting an insulation material, e.g. aramid paper.

Figure 47 Slots insulation (Carnevale, 2020)

3- Insert the hairpin coils into the rectangular slots.

4- Once the coils are inserted, their ends must be twisted and welded as shown in the following figure.
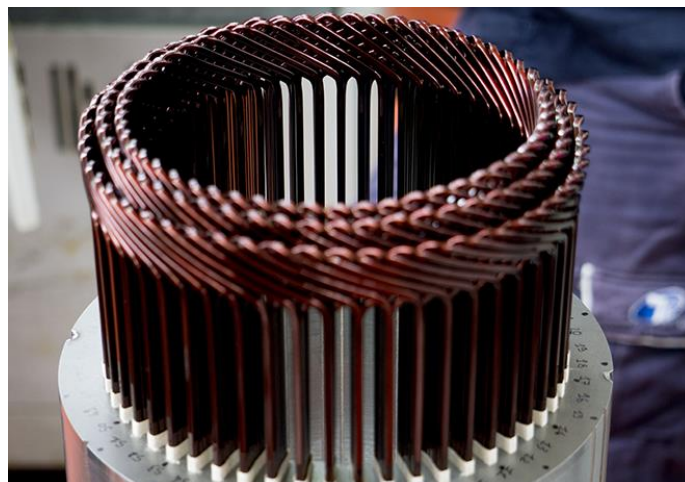
Figure 48 Final assembly of hairpin winding (Kent, 2018)

7.1.4 Permanent magnet insertion

Once the rotor core is stacked and welded the permanent magnets are inserted into the rotor slot, in this step, much attention must be paid to the magnetization direction of the magnets, the magnets must be magnetized through the thickness and then inserted in the rotor slots as illustrated in the figure50 to form the rotor poles.

The figure51 shows the flux direction in the rotor of PMSM simulated by FEMM software.
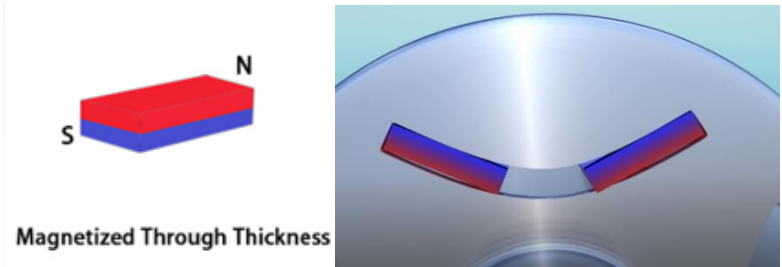
Figure 49 Magnets magnetization.
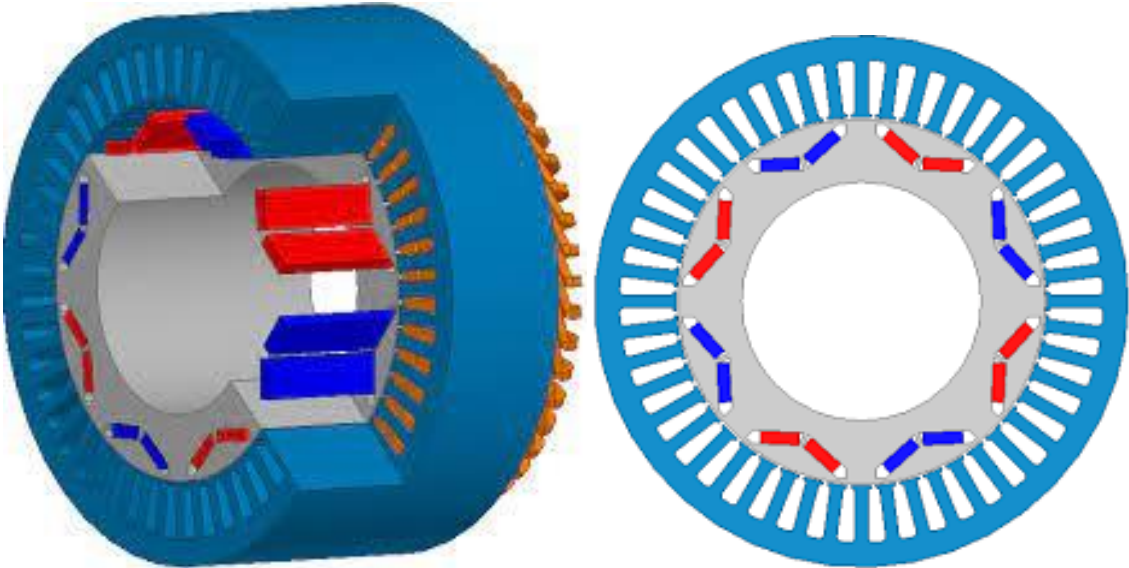
Figure 50 Magnet insertion.
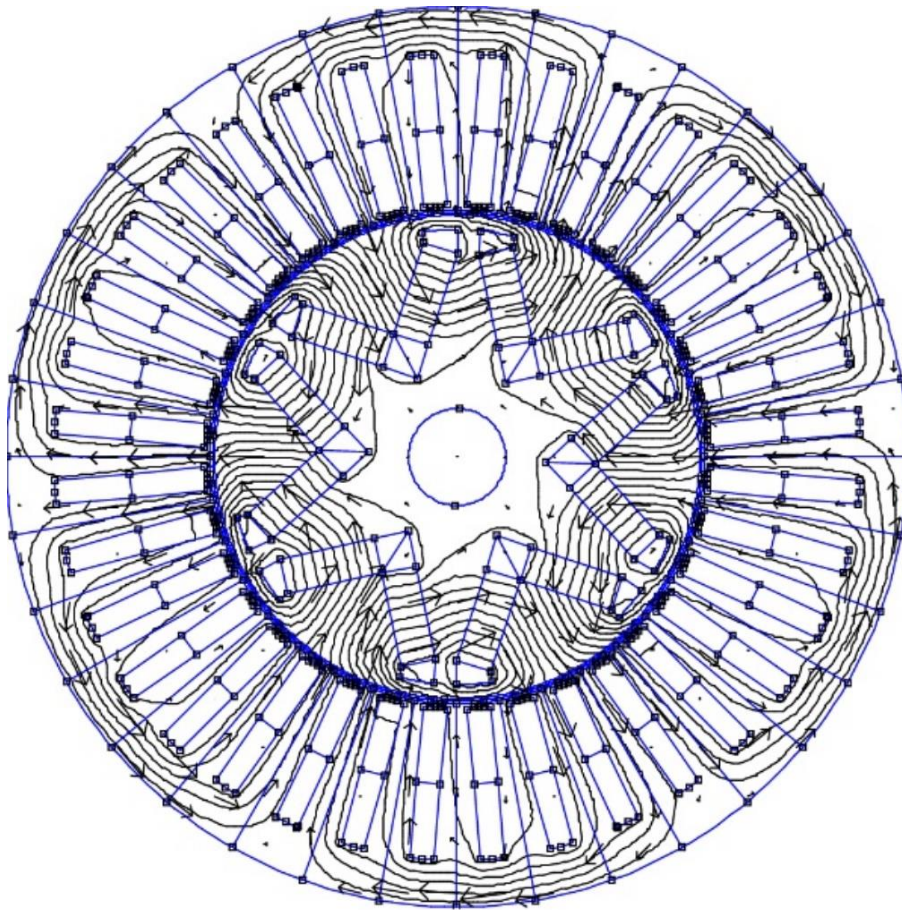
Figure 51 Magnetic flux direction.

7.2 **Prototype tests**

The aim of performing tests and measurements on the prototype is to verify the results from the simulations software but also to learn more about the machine performance, the designer gains valuable experience by performing the tests in the lab.

This chapter discusses tests that can be performed to obtain the steady-state characteristics of PMSM. The steady-state tests can be characterized as the open-circuit test, short-circuit test, and load operation test (IEEE, 2021).

Open circuit

Open circuit tests are performed with no current flowing in the stator winding, and by running the machine with a constant speed

Open-Circuit Voltage(Emf)

The open-circuit voltage is the induced EMF, it depends on the residual flux density and the coercivity, of the permanent magnets, which are temperature-dependent. For example, both the residual flux density and coercivity of rare-earth magnet materials such as neodymium-iron-boron are inversely proportional to the temperature.

Since the open-circuit voltage depends on the PMs parameters and the lasts are temperature depending, temperature measurement is necessary, the temperature measurements of rotating magnets are difficult to perform without specialized instrumentation (e.g., a telemetry system). But if the machine is tested in thermal steady-state conditions the open-circuit voltage can be determined.

The open-voltage test is not performed only to determine the EMF value but also to measure its balance and harmonic content. And as it was mentioned before by having the PMs parameters which are temperature-dependent characteristics, the open-circuit voltage measurement can be an indirect indication of the magnet temperature.

Test predecessor:

- Since the open-circuit test is performed with no current in the stator winding, the machine is driven by a driving motor at a constant speed as illustrated in figure52.

- The test is performed in a thermal steady state condition therefore the machine winding temperature should be measured and monitored to ensure the thermal in steady-state conditions.

- Once a steady-state condition has been reached, the voltage balance must be checked by measuring all line-line voltages to ensure that the voltages don't have any unbalance in magnitude and phase.

  Digital or analogue meters can be used to measure their values (rms voltage). A Digital scope or data acquisition system are also used to obtain details of the voltage waveforms so the harmonic content can be analyzed, and other characteristics of the voltage waveforms.

- The open-circuit voltage depends on the machine speed, therefore the speed should be measured simultaneously with the voltage, a tachometer can be used to measure the machine speed.
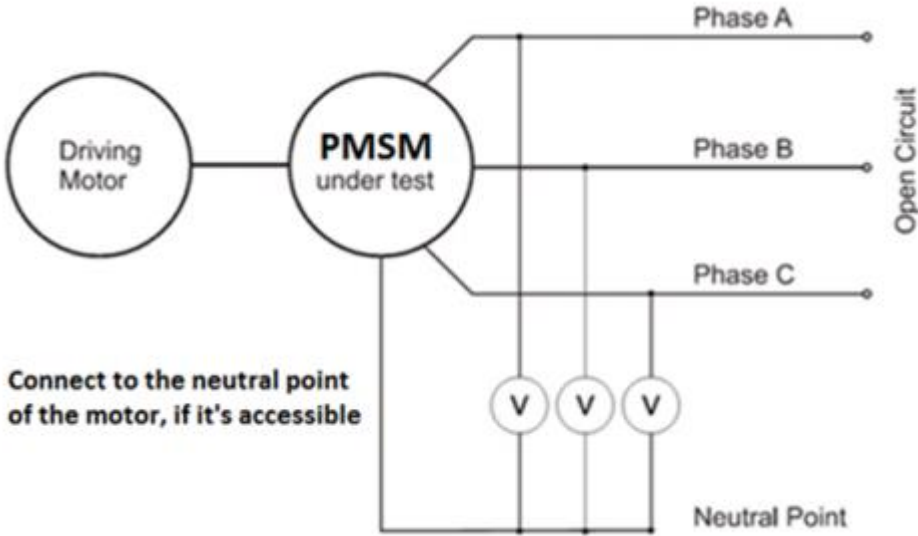
Figure 52Three-phase measurement of the open-circuit voltage(EMF)

Open Circuit Losses

Open circuit tests are used to determine machine losses such the friction losses and the windage losses under open-circuit conditions, two important parameters must be taken into account in this test which is the machine speed and the operational temperature, the friction losses are affected by the machine speed and the windage losses are affected by the temperature.

The friction losses and winding losses in open circuit conditions are determined by measuring the power input to the machine with no excitation in the rotor, therefore the test is performed by replacing the PMSM rotor with a (non-magnetized) equivalent rotor. This can be performed by applying one of the following methods:

a) Using the same rotor with the magnets not yet to be magnetized.

b) Using the same rotor but without the magnets, and in the rotor slots filled with non-magnetized material.

Test predecessor:

- Once the equivalent rotor is installed, a drive motor used to run the machine at the desired speed.

- There are two ways to measure the combined friction and windage loss (directly or indirectly methods):

a) In the direct method, the torque and power are directly measured by torque transducer placed between the drive motor and the PMSM which measure the friction and windage loss torque (TFW) then the corresponding power loss (PFW)can be calculated as follows:

$$PFW = \omega_m TFW \qquad 7\text{-}1$$

Where ω_m, is the test speed.
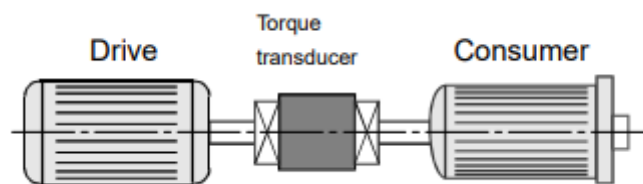
Figure 53 Direct torque measurement. (Schicker & Wegener, s.f.)

b) The indirect measurement can be performed by measuring the input/ powers, the test starts by running the machine with the drive motor at the test speed, If the drive-motor loss (Ploss, drive) can accurately be determined, the PFW can be obtained as follows:

$$PFW = Pdrive - Ploss, drive$$

Where $Pdriv$, is the drive-motor input power.

Cogging torque

PMSM for automotive applications requires low torque ripple due to the vibration and acoustic noise problem produced by high values of torque ripple.

During the measurement of cogging torque, it's important to note that cogging torque may cause variations in rotor speed during the machine rotation. Therefore, cogging torque measurements are performed statically torque measurements(zero speed). or dynamically with very low and constant motor speed.

Test predecessor:

Cogging torque can be measured dynamically as illustrated in Figure.54 or statically as Figure.55.

To perform the static measurement shown in Figure 2 a circular indexing fixture calibrated in mechanical degrees is required, which is incremented in discrete steps.

The torque is measured after each rotation and after a sufficient number of measures, the cogging torque is obtained. The static measurements are performed in open circuit conditions with no excitation.
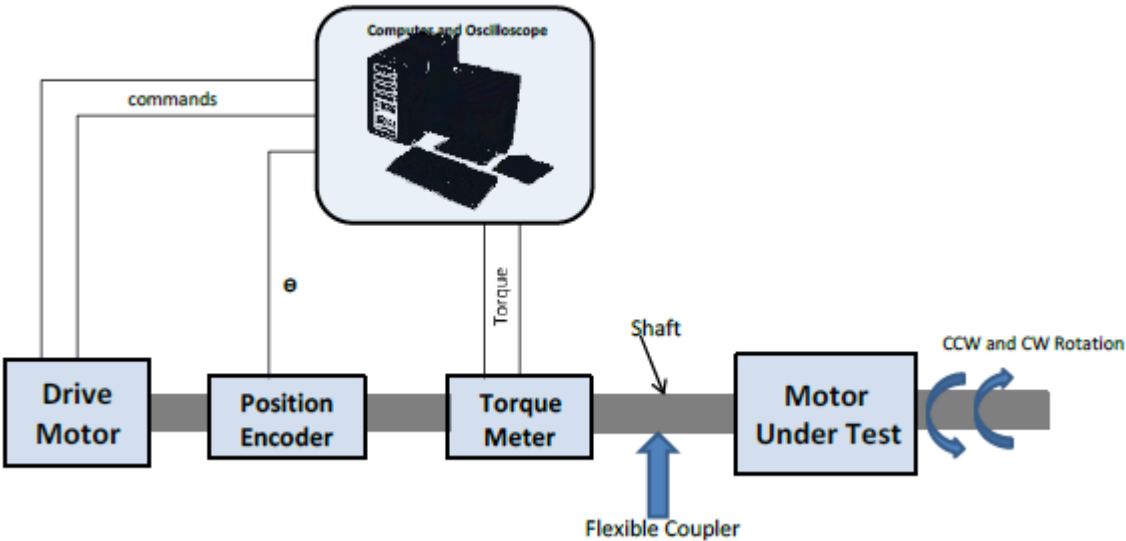
Figure 54 Schematic to dynamically measure cogging torque *(IEEE, 2021).*
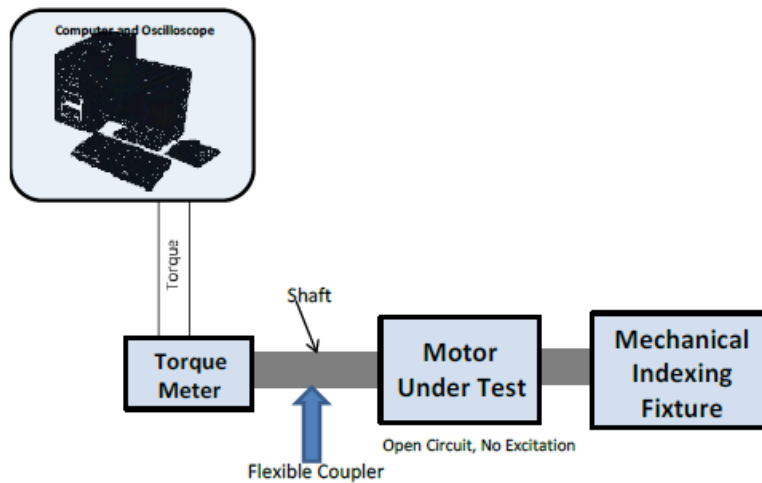
Figure 55 Schematic to statically measure cogging torque of a PM machine (IEEE, 2021).

Short-circuit tests

The short circuit test is used to determine the stator current which is used to calculate the direct-axis reactance of the PMSM. While the measured temperature in steady-state short-circuit conditions is used to determine the thermal performance of a PMSM and its cooling system.
As the open circuit tests, the realized measure in the short circuit test is also temperature depending, and it will vary depending on the PMs temperature.
The test is performed by short-circuited the machine stator terminals as illustrated in Figure 56, The machine is driven by a drive motor and an external current-limiting impedance in series with each winding phase is used to limit the temperature rise. This impedance should be a reactive impedance since the resistive cause increasing in the machine losses.
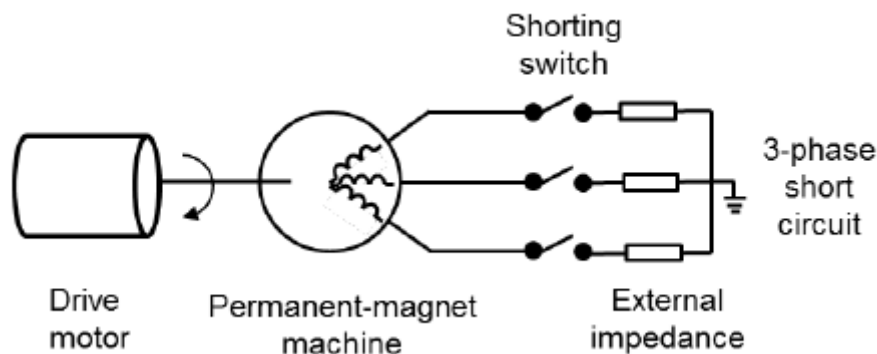
Figure 56 Short-circuit test configuration (IEEE, 2021)

Test predecessor:

To determine the synchronous inductance (d-axis synchronous inductance) in shot-circuit conditions, the following steps must be performed:

a) the open-circuit voltage must be measured as mentioned before.

b) run the PMSM with the drive motor to the desired test speed.

c) once the test speed is reached, the short circuit current is measured and by applying the following equation, the synchronous inductance is determined:

$$I_{sc} = \frac{V_{oc}}{\sqrt{3}X_{sc}}$$

Where:

- I_{sc}: Short-Circuit Current.

- V_{oc}: Open-Circuit Voltage.

- X_{sc}: Short-Circuit Inductance.

Load tests

The load tests are performed to check the machine performance at the operating conditions for which they are designed. The machine performance is characterized and studied by the determination of the machine performance parameters such as efficiency, power factor, machine temperature, voltage and current balance and harmonic distortion as well as vibration, and acoustic noise.
The load tests measured parameters are also temperature-dependent as in the open and the short circuit tests therefore the tests must be performed while the temperature is continually monitored by temperature sensors to verify that the machine is operating under steady-state conditions when measurements are made.

Test predecessor:

PMSMs can be supplied from a variable-frequency inverter or a fixed or variable-frequency, sinusoidal source.

If the supplier is a variable-frequency source, the test procedure is as follows:
- A drive motor is used to run the PMSM to the test speed.
- Adjust the applied voltage and motor load to the test level.
- Assure a thermal steady state by monitoring the temperature.
- Measurements appropriate to the test objectiveS can be made. The measurements include voltages, currents, power, torque, temperature, and vibration. And the used instruments to perform the tests are listed later in this chapter.

If the supplier is a fixed frequency, sinusoidal source, the test procedure is as follows:
- The motor is running with synchronous speed by using a load motor is used.
- The fixed frequency source should be connected to the PMSM.
- The terminal voltage should be adjusted to the test conditions.
- The load is next adjusted to the desired test level.
- Assure a thermal steady state by monitoring the temperature.
- Measurements appropriate to the test objectiveS can be made. The measurements include voltages, currents, power, torque, temperature, and vibration. And the used instruments to perform the tests are listed later in this chapter.

Instrumentation

the used instruments depend on the objective of the tests and what parameters to be obtained from the test, the used instruments are listed in the following list:

- Terminal voltage and current Instrumentation. Simple analogue meters can be used but for more detailed measurements an oscilloscope or data acquisition system can be used.
- Electrical power Instrumentation.
- A torque transducer to measure shaft torque.
- Machine speed Instrumentation. two ways can be used to obtain the speed, directly by using the tachometer and indirectly by measuring the frequency of the terminal voltage then calculating the speed.
- Temperaturas Instrumentation.
- Vibration Instrumentation.
- If a special cooling system is applied, it may be used instrumentation to monitor the performance of the cooling system and its impact on the machine performance.

8 Discussion and Conclusions

Throughout this thesis, a PMSM was designed and simulated by FEMM software, assembly instruction and tests guide were designed to verify the machine performance.

It has been satisfactorily verified that the final prototype meets the machine specifications and with very high efficiency, around 98%.

The machine was first modelled by the analytical method and an approximation of the machine model was obtained, then through the Finite Element Method, accurate parameters were obtained and the final design was selected. After the FEA was performed the results were compared to the analytical results and they were similar

Due to the lack of time and due to the large delivery time of the materials, the manufacturing process and the prototype building is not complete, therefore the tests and assembly instructions were designed but not performed yet on the prototype.

9 Future work

Following the conclusions found in the previous chapter, the efficiency advantages of the permanent magnet synchronous motor were demonstrated. However, based on this work, new lines of improvement and study can be devised that allows the full potential of this motor morphology to be exploited.

- Three-dimensional analysis: The two-dimensional study of the prototype is enough to get a fairly approximate idea of the real response of the engine. However, a three-dimensional analysis allows one to analyze the phenomena in the direction of the motor shaft. Although these phenomena are considered minimal compared to those analyzed in two dimensions, they allow a more precise study of the prototype.
- Thermal analysis which allows the studying of the operating temperature of the elements of the machine, checking if their maximum limits are not reached and that the integrity of the motor is not compromised, a lumped circuit could be created and tested by MOTOR-CAD, or by using the thermal analysis of FEMM.
- A genetic algorithm optimization could be implemented to optimize the design.
- PM losses model could be implemented in FEMM.
- A mechanical analysis can be implemented which allows the studying of the stress states to which the different parts of the engine are subjected. It is especially interesting in the case of magnets, which are the most fragile element in the motor.
- Investigate new materials: Analyze possible alternatives to the ferromagnetic sheet used to reduce iron losses; as well as other possible magnets with better magnetic or mechanical properties.

10 References

Berman, G. A., 1979. *Testing Laboratory Performance: Evaluation and Accreditation.* Washington: National Bureau of Standards.

Bianchini, C. o.a., 2020. Slot Design Optimization for Copper Losses Reduction in Electric Machines for High-Speed Applications. *applied sciences,* p. 16.

Carnevale, N., 2020. Aislamiento de Motores Eléctricos de Baja Tensión – Aislamiento de la Máquina. *motoresygeneradores.com*.

Chau, K. T., 2015. *Electric Vehicle Machines and Drives.* Singapore: Wiley.

Chau, K. T., Chan, C. C. & Chunhua, L., 2008. Overview of Permanent-Magnet Brushless Drives for Electric and Hybrid Electric Vehicles. *IEEE,* p. 12.

chile, E. l. r. e. d., 2017. Motores de reluctancia: opción de menor consumo eléctrico para minería. *https://www.revistaei.cl/informes-tecnicos/motores-reluctancia-opcion-menor-consumo-electrico-mineria/*, 10 Abril.

Collins, D., 2018. Hysteresis loss and eddy current loss: What's the difference?. *https://www.motioncontroltips.com/*, 30 March.

Deurell, D. & Josefsson, V., 2019. *FEA study of proximity effect in hairpin windings of PMSM for automotive applications,* Gothenburg: CHALMERS UNIVERSITY OF TECHNOLOGY.

DistriMotor, 2020. Cómo funciona un motor asíncrono trifásico. *https://www.distrimotor.es/*.

Fernández, F. J. M., 2014. *Electric traction machine design for an E-RWD unit,* Lund: Lund University.

Fleisch, D., 2008. *A Student's Guide to Maxwell's Equations.* New York: Cambridge University Press.

Gieras, J. F. & Wing, M., 2002. *Permanent Magnet Motor Technology.* Basel: Marcel Dekker AG.

Hanselman, 1994. *DC Brushless Permanent-Magnet Motor Design.* New York: McGraw-Hill.

Hanselman, D., 2006. *Brushless Permanent Magnet Motor Design.* Ohio: Magna Physics Publishing.

Hendershot, J. J. & Miller, T., 1994. *Design of Brushless Permanent-Magnet Machines.* Oxford: Magna Physics Publications, Oxford Science Publications.

Huijuan , L., Jingxiong , Z. & Zhang, H., 2013. PM Design of IPMSM using Parameterized Finite Element Model. *TELKOMNIKA,* p. 9.

IEEE, I. P. a. E. S., 2021. IEEE Trial-Use Guide for Testing Permanent Magnet Machines. *IEEE Power and Energy Society,* p. 56.

Jagasics, S. & Vajda, I., 2016. Comparison of different PMSM rotor configurations. *Reaserch Gate,* p. 5.

Jape, S. R. & Thosar, A., 2017. COMPARISON OF ELECTRIC MOTORS FOR ELECTRIC VEHICLE APPLICATION. *International Journal of Research in Engineering and Technology,* p. 6.

Josselin, J. M. & Le Maux, B., 2017. *Statistical Tools for Program Evaluation.* Switzerland: Springer International Publishing AG.

Kent, M., 2018. Tecnomatic helps automakers design specialty assembly processes for advanced stator technologies. *CHARGED ELECTRIC VEHICLE MAGAZINE* , June, p. 5.

Kothari, D. P. & Nagrath, I. J., 2010. *Electric Machines.* New Delhi: McGraw-Hill.

Krings, A., Nategh, S., Wallmark, O. & Soulard, J., 2014. Influence of the Welding Process on the Performance of Slot-less PM Motors with SiFe and NiFe Stator Laminations. *IEEE Transactions on Industry Applications,* p. 11.

Levkin, D., u.d. Permanent magnet synchronous motor. *https://en.engineering-solutions.ru/motorcontrol/pmsm/.*

Limited, M. D., 2021. Maximising E-Machine Effciency with Hairpin Windings. *motor-design.com*, p. 7.

Lin, R., 2017. *A DESIGN PARADIGM FOR V-SHAPE INTERIOR PERMANENT-MAGNET MACHINE USING MULTI-OBJECTIVE OPTIMIZATION,* Indiana: Purdue University.

LowCVP, 2015. [Online]
Available at: https://www.zemo.org.uk/assets/workingdocuments/MC-P-11-15a%20Lifecycle%20emissions%20report.pdf

MARTÍNEZ, D., 2012. *Design of a Permanent-Magnet Synchronous Machine with Non-Overlapping Concentrated Windings,* Stockholm: u.n.

Mechatronics, H. t., 2019. How Brushless Motor and ESC Work. *https://howtomechatronics.com/how-it-works/how-brushless-motor-and-esc-work/.*

Miller, T. J. E., 1989. *Brushless Permanent Magnet and Reluctance Motor Drives.* New York: Oxford University Press.

Murali, N., Ushakumari, S. & V.P, M., 2020. *Performance comparison between different rotor configurations of PMSM for EV application.* Osaka, IEEE REGION 10 CONFERENCE (TENCON).

Namitha, M., S., U. & Mini, V., 2020. Performance comparison between different rotor configurations of PMSM for EV application. *IEEE,* p. 6.

Nasar, S. A., Boldea, I. & Unnewehr, L., 1993. *Permanent Magnet, Reluctance, and Self-Synchronous Motors.* Boca Raton: CRC Press.

Nogueira, A., 2013. PRACTICAL ISSUES ON THE MODELING OF PERMANENT-MAGNET MACHINES AND COGGING TORQUE CALCULATIONS IN TWO- DIMENSIONAL FINITE-ELEMENT ANALYSIS. *Research Gate,* p. 8.

Piccoli, M. & Yim, M., 2016. Anticogging: Torque Ripple Suppression, Modeling, and Parameter Selection. *The International Journal of Robotics Research,* p. 13.

Pyrhonen, J., Jokinen, T. & Hrabovcova, V., 2008. *Design of rotating electrical machines.* u.o.:John Wiley & Sons.Ltd.

Qinghua, L., 2005. *ANALYSIS, DESIGN AND CONTROL OF PERMANENT MAGNET SYNCHRONOUS MOTORS FOR WIDE-SPEED OPERATION,* u.o.: National University of Singapore.

Sarrico, J. G. V. V., 2017. *Design and implementation of a 20 kW, 12000 RPM Permanent Magnet Synchronous Motor (PMSM) for the IST Formula Student Powertrain,* u.o.: u.n.

Sarrico, J. G. V. V., 2017. *Design and Implemntation of a 20 kW, 12000 PRM Permanent Magnet Synchronous Motor (PMSM) for the IST Formula Student Powertrain,* u.o.: u.n.

Schicker, R. & Wegener, G., u.d. Measuring Torque Correctly. *https://www.hbm.com/en/0080/torque-measurement/,* p. 261.

Spektrumrc, 2021. Brushless Motor. *http://spektrumrc.com/Products/Default.aspx?ProdID=SPMXSM1000*, June.

Wenmin, S., Jing, L. & Changyi, L., 2014. Effect of Cutting Techniques on the Structure and Magnetic Properties of a High-grade Non-oriented Electrical Steel. *Journal of Wuhan University of Technology-Mater. Sci. ,* p. 6.

Wildi, T., 2002. *Electrical Machines Drive, and Power System.* New Jersey: Pearson Education.

Appendices

List of Figures

List of tables